# THE LATERAL-TORSIONAL BUCKLING OF DOUBLY SYMMETRIC WIDE FLANGE SECTIONS

by

RONALD H. DE VALL

B.A.Sc. (Civil Eng.)

The University of British Columbia, 1966

A THESIS SUBMITTED IN PARTIAL FULFILMENT OF

THE REQUIREMENTS FOR THE DEGREE OF

MASTER OF APPLIED SCIENCE

in the Department

of

CIVIL ENGINEERING

We accept this thesis as conforming
to the required standard

THE UNIVERSITY OF BRITISH COLUMBIA

March, 1968

In presenting this thesis in partial fulfilment of the requirements for an advanced degree at the University of British Columbia, I agree that the Library shall make it freely available for reference and study. I further agree that permission for extensive copying of this thesis for scholarly purposes may be granted by the Head of my Department or by his representatives. It is understood that copying or publication of this thesis for financial gain shall not be allowed without my written permission.

R. H. De Vall

Department of Civil Engineering

The University of British Columbia
Vancouver 8, B.C.

March 1968

# ABSTRACT

In this thesis, a stiffness matrix which includes the non-linear effects of principal plane shears, moments and axial loads on lateral and torsional deflections is developed for a doubly symmetric wide flange section.

Initially, an exact eight by eight linear matrix is developed for an element of constant section properties. The eight allowable deflections allows the independent representation of the deflections of either flange at either end. The non-linear effects are included in the differential equations by considering the effect of the primary stresses on the equilibrium of a displaced element.

Two approximations are then introduced. The first consists of a numerical technique for solving the differential equations. The second consists of a simplification of the boundary conditions in solving the differential equations. Using these two approximations, the non-linear portion of the matrix is then built.

Several structures are then analyzed. Each structure is divided into several elements. This allows beams of non-constant section properties to be analyzed, and increases the accuracy of the results of the approximate matrices.

The results of these analyses are then compared to theoretical results and tabulated. It is seen that the matrix gives good agreement for all cases tested.

TABLE OF CONTENTS

# LIST OF FIGURES

LIST OF FIGURES (Contd.)

# DEFINITION OF SYMBOLS

$I$ = moment of inertia of flange about strong axis

$I_z$ = moment of inertia of section about z axis

$I_y$ = moment of inertia of section about y axis

$I_p$ = polar moment of inertia

$A$ = area of section

$A_w$ = area of web

$J$ = torsional constant

$E$ = Youngs modulus

$G$ = shear modulus

$C$ = $JG$

$h$ = depth of section

$\alpha^2$ = $2C/EIh^2$

$y$ = lateral deflection (along y axis)

$z$ = vertical deflection (along z axis)

$\phi$ = torsional deflection

$Q$ = flange shear

$T$ = torque

$\omega$ = distributed load

$q$ = distributed torque

$\delta_n$ = stiffness matrix deflection in n direction

$f_n$ = stiffness matrix force in n direction

$L$ = length of element

$P$ = principal axial load in element

$M_o$ = principal moment at ¢ of element

$V$ = principal shear in element

$M$ = $M_o - VL/2 + Vx$ = moment in element @ point x

$\sigma$ = normal stress in element

## DEFINITION OF SYMBOLS (Contd.)

$M_f$ = flange moment

$\sigma_o$ = P/A

$\tau$ = shear stress in element

$p$ = pressure due to n stresses

$\lambda$ = $M_o/2EI$ = parameter in solution expansion

$y_n$ = $n^{th}$ term in series solution of y

$\phi_n$ = $n^{th}$ term in series solution of $\phi$

$\eta$ = dummy integral parameter

$\rho$ = dummy integral parameter

$\xi$ = dummy integral parameter

$'$ = differentiation with respect to x

R.H.S Right hand side

L.H.S Left hand side

# ACKNOWLEDGEMENTS

The author wishes to thank his supervisor, Dr. R. F. Hooley, for his invaluable assistance and encouragement during the development of this work. Gratitude is also expressed to the National Research Council of Canada for financial support, and to the U.B.C. Computing Center for the use of its facilities.

March 1968

Vancouver, B.C.

# THE LATERAL-TORSIONAL BUCKLING OF DOUBLY SYMMETRIC WIDE FLANGE SECTION

## CHAPTER I

## INTRODUCTION

The lateral torsional buckling of beams has been a topic of interest and research for years. The foundations of the theory of lateral torsional buckling of thin rectangular sections were laid by Prandtl and Michelle [5, 6][a] in 1899 in the study of the lateral buckling of thin rectangular sections. H. Reissner [6] later stressed the effect of deflections in the major principal axis in the Prandtl-Michelle theory and introduced modifications to account for them. In 1910, S. Timoshenko [1] developed the differential equation that included the warping effect of the flanges of I sections deformed in torsion. In 1929, Wagner [6] determined that thin open sections may buckle in a pure torsional mode under an applied axial load.

Since then many other researchers have contributed to the knowledge of lateral buckling. The usual form this work has taken is the direct solution of the differential equation for simple cases and the use of numerical methods in the more complicated cases. The drawback in the above approaches is the difficulty in applying them to the general case. As the complexity of the load and support conditions increases, the problem becomes intractible.

The purpose of this thesis will be the presentation of a method for the elastic analyses of lateral torsional buckling of doubly symmetric wide flange sections under principal moment, shear and axial loads. The method of solution utilizes a stiffness matrix consisting of two parts - an exact elastic linear portion and an approximate non-linear portion. The matrix is developed

---

[a] Numbers in square brackets refer to the References.

using the assumptions that deflections in the principal plane remain small, the stresses remain elastic, there is no distortion of the cross-section, and the loads maintain their original direction of application. These matrices, once obtained, can be used to build any case of varying support, fixity and load conditions of beams with varying section properties.

# CHAPTER II

## DEVELOPMENT OF LINEAR MATRIX

In order to develop a stiffness matrix, the governing differential equations of the section must first be obtained.

For the development of the linear case differential equations, a right-handed co-ordinate system was used as in Fig. 1(a), with the usual bending moment-shear sign convention used for bending of the top flange, as in Fig. 1(b). Rotation producing positive y deflection of the upper flange was chosen as positive as shown in Fig. 1(c). A positive end torque T induces positive pure torsion in the section and a negative shear in the top flange.

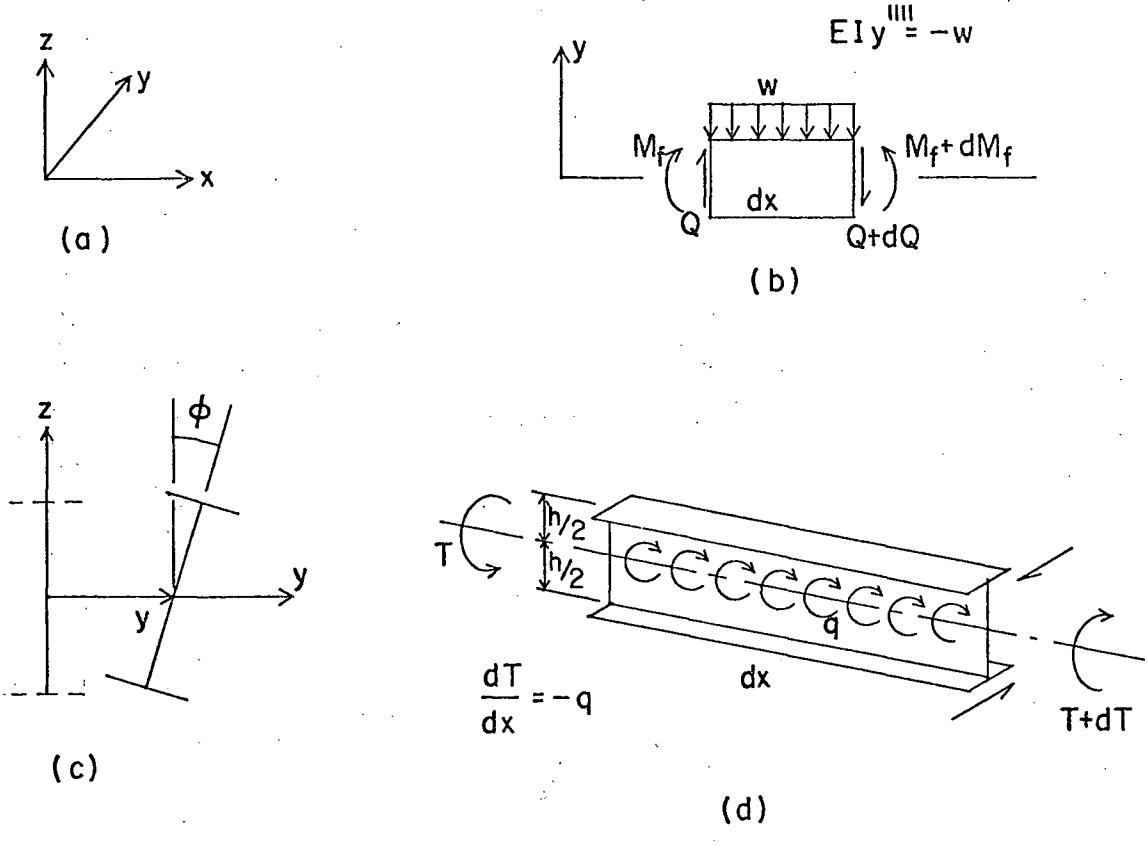


Fig. 1 SIGN CONVENTIONS

To obtain the differential equation for torsion, it is only necessary to consider the applied torque at any point along the section. The torque due to shear in the flange is $= - Vh = - (h\phi'''/2)(EIh) = -\phi''' EIh^2/2$. The torque due to pure torsion is $C\phi'$. Therefore the equation for torque T acting at any section is

$$C\phi' - \frac{EIh^2}{2}\phi''' = T \qquad (1)$$

as first developed by Timoshenko [1].

Equation (1) reduces to

$$\phi''' - \alpha^2\phi = -\frac{\alpha^2 T}{C} \qquad \text{where } \alpha^2 = \frac{2C}{EIh^2}$$

One integration gives

$$\phi'' - \alpha^2\phi = -\frac{\alpha^2 T}{C}[x + A] \qquad (2)$$

To obtain the equation of the section under the action of a distributed torque, equation (1) is differentiated once to give

$$C\phi'' - \frac{EIh^2}{2}\phi'''' = T' = -q \qquad (3)$$

The equation governing pure lateral deflection is the well known

$$2EIY'''' = -\omega \qquad (4)$$

Rather than solve equations (2) and (4) for any condition of load or variation of section properties, it is better to split the beam into a number of segments; each segment having constant section properties, torques and lateral shears. The solution of equations (2) and (4) for such a segment will be relatively simple, and a stiffness matrix for the segment can easily be built. By utilizing several elements to represent a structure under distributed load or varying section properties, very little accuracy will be lost.

The segment used is shown in Fig. 2.

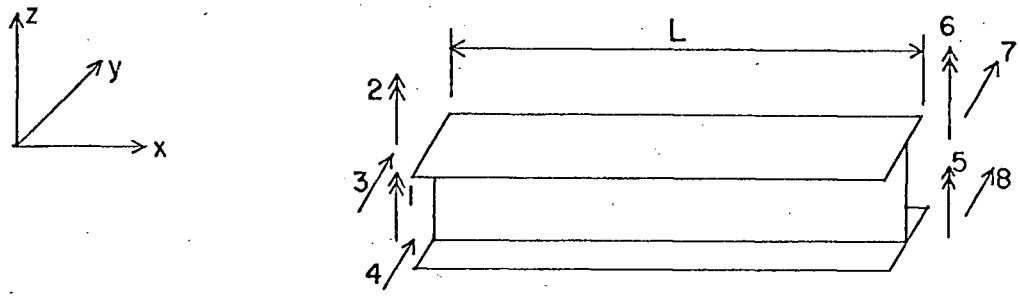


Fig. 2 BEAM SEGMENT

In this figure, torsional deflections and forces are accounted for indirectly through the differences in lateral shear deflection and forces. The relationship between the eight independent deflections and their corresponding forces are given by $k\delta = f$ where $\delta$ is an 8×1 matrix representing the deflections $\delta_1, \ldots \delta_8$, f is an 8×1 matrix representing the forces $f_1, \ldots f_8$, and k is an 8×8 matrix joining the two. By examining the segment in Fig. 2, and using Fig. 1(c), the following relations are obtained.

$$
\left.\begin{aligned}
\delta_1 &= y' - \phi' h/2 \\
\delta_2 &= y' + \phi' h/2 \\
\delta_3 &= y + \phi\, h/2 \\
\delta_4 &= y - \phi\, h/2
\end{aligned}\right\} x = 0
\qquad
\left.\begin{aligned}
f_1 &= -EI(y'' - \phi''\, h/2) \\
f_2 &= -EI(y'' + \phi''\, h/2) \\
f_3 &= +EI(y''' + \phi'''\, h/2) - C\phi'/h \\
f_4 &= +EI(y''' - \phi'''\, h/2) + C\phi'/h
\end{aligned}\right\} x = 0
$$

$$
\left.\begin{aligned}
\delta_5 &= y' - \phi' h/2 \\
\delta_6 &= y' + \phi' h/2 \\
\delta_7 &= y + \phi\, h/2 \\
\delta_8 &= y - \phi\, h/2
\end{aligned}\right\} x = L
\qquad
\left.\begin{aligned}
f_5 &= +EI(y'' - \phi''\, h/2) \\
f_6 &= +EI(y'' + \phi''\, h/2) \\
f_7 &= -EI(y''' + \phi'''\, h/2) + C\phi'/h \\
f_8 &= -EI(y''' - \phi'''\, h/2) - C\phi'/h
\end{aligned}\right\} x = L
\qquad (5)
$$

If $k_{8\times 8}$ were obtained by allowing $\delta_n = 1$, with all other $\delta$'s equal to zero, the calculations would entail working with combined bending and torsion. It is therefore proposed to solve four basic pure bending cases and four basic pure torsional cases which can be superposed to give any desired deflected shape. The four of these modes associated with the right hand end deflections are given in Fig. 3.

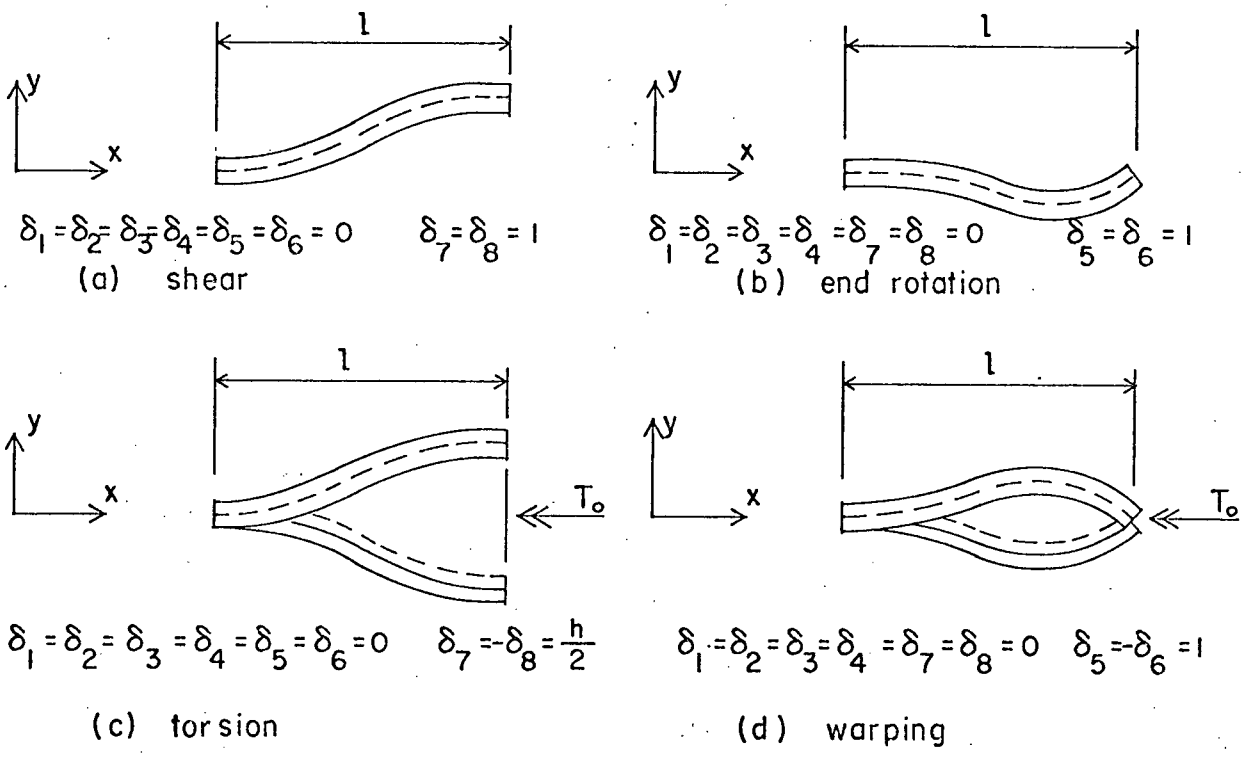


Fig. 3 PRIMARY MODES FOR RIGHT HAND END DEFLECTIONS

The shapes in Fig. 3(a), (b) are solved using eq.(4). Since their solution gives the well known beam stiffness equations, they will not be gone into in further detail. The shapes presented in Fig. 3(c), (d) are torsional shapes and can be solved using eq.(2).

The shape in Fig. 3(c) represents a unit torsional rotation with all other allowable deflections fixed. The end conditions for this case are:

$x = 0 \quad \phi = 0 \qquad\qquad x = L \quad \phi = 1$

$\phi' = 0 \qquad\qquad \phi' = 0$

The solution of eq.(2) for this case is

$$\phi = B_o \sinh \alpha x + D_o \cosh \alpha x + \frac{T_o}{C}[x + A]$$

where $B_o = -\frac{T_o}{\alpha C} \quad D_o = \frac{T_o(\cosh \alpha L - 1)}{C\alpha \sinh \alpha L} \quad A_o = -\frac{(\cosh \alpha L - 1)}{\alpha \sinh \alpha L}$ (6)

$$T_o = \frac{\alpha C \sinh \alpha L}{[2-2\cosh \alpha L + \alpha L \sinh \alpha L]}$$

The shape in Fig. 3(b) is obtained by applying equal and opposite moments to the upper and lower flanges of one end, and restraining all other allowable deflections. The end conditions for this case are:

$x = 0 \quad \phi = 0 \qquad\qquad x = L \quad \phi = 0$

$\phi' = 0 \qquad\qquad \frac{\phi' h}{2} = -1$

The solution of eq.(2) for this case is:

$$\phi = B_1 \sinh \alpha x + D_1 \cosh \alpha x + \frac{T_1}{C}[x + A_1]$$

where $B_1 = -\frac{T_1}{C\alpha} \quad D_1 = -\frac{T_1}{C}\left[\frac{\sinh \alpha L - \alpha L}{\alpha(1 - \cosh \alpha L)}\right] \quad A_1 = \frac{\sinh \alpha L - \alpha L}{\alpha(1 - \cosh \alpha L)}$ (7)

$$T_1 = -\frac{2C}{h}\left[\frac{1 - \cosh \alpha L}{[2-2\cosh \alpha L + \alpha L \sinh \alpha L]}\right]$$

Using the above solutions, the individual columns of the stiffness matrix may be obtained by superposition. As an example, columns 6 and 7 can be obtained by using the shapes in Fig. 3 as indicated in Fig. 4.

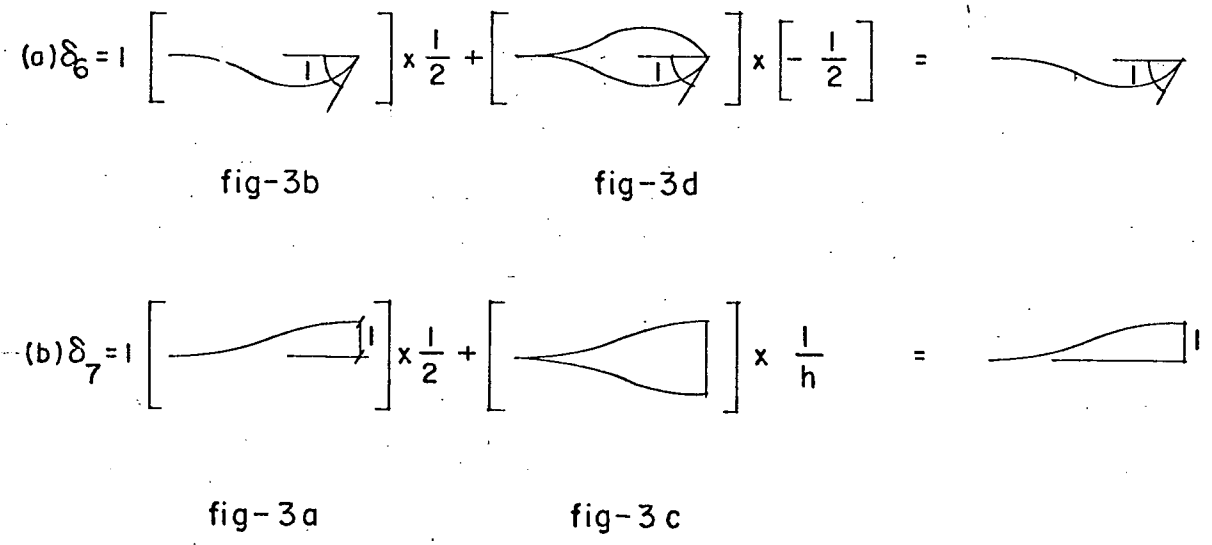


Fig. 4 SUPERPOSITION OF PRIMARY MODES

Similar operations yield the other columns of the stiffness matrix.

Presentation of the matrix is simplified by introducing the following functions.

$$S_1 = (\alpha L)^3 \sinh \alpha L/12\phi$$

$$S_2 = (\alpha L)^2 (\cosh \alpha L - 1)/6\phi$$

$$S_3 = \alpha L (\alpha L \cosh \alpha L - \sinh \alpha L)/4\phi$$

$$S_4 = \alpha L (\sinh \alpha L - \alpha L)/2\phi$$

$$\phi = 2\text{-}2 \cosh \alpha L + \alpha L \sinh \alpha L$$

$$\alpha^2 = 2C/EIh^2$$

where $S_1$, $S_2$, $S_3$, $S_4$ and $\phi$ are the same as the stability functions given in Gere and Weaver.[2] Use of these functions to represent the forces gives the complete linear matrix $K_o$, shown in Fig. 5.

$$K_o = \frac{EI}{L^3}$$

| | 1 | 2 | 3 | 4 | 5 | 6 | 7 | 8 |
|---|---|---|---|---|---|---|---|---|
| 1 | $2L^2[1 + S_3]$ | | | | | | | |
| 2 | $2L^2[1 - S_3]$ | $2L^2[1 + S_3]$ | | | | | | |
| 3 | $3L[1 - S_2]$ | $3L[1 + S_2]$ | $6[1 + S_1]$ | | SYMMETRIC | | | |
| 4 | $3L[1 + S_2]$ | $3L[1 - S_2]$ | $6[1 - S_1]$ | $6[1 + S_1]$ | | | | |
| 5 | $L^2[1 + S_4]$ | $L^2[1 - S_4]$ | $3L[1 - S_2]$ | $3L[1 + S_2]$ | $2L^2[1 + S_3]$ | | | |
| 6 | $L^2[1 - S_4]$ | $L^2[1 + S_4]$ | $3L[1 + S_2]$ | $3L[1 - S_2]$ | $2L^2[1-S_3]$ | $2L^2[1 + S_3]$ | | |
| 7 | $3L[-1 + S_2]$ | $3L[-1 - S_2]$ | $6[-1 - S_1]$ | $+6[-1 + S_1]$ | $3L[-1 + S_2]$ | $3L[-1 - S_2]$ | $6[1 + S_1]$ | |
| 8 | $3L[-1 - S_2]$ | $3L[-1 + S_2]$ | $6[-1 + S_1]$ | $6[-1 - S_1]$ | $3L[-1 - S_2]$ | $+3L[-1 + S_2]$ | $6[1 - S_1]$ | $6[1+S_1]$ |

Fig. 5 LINEAR STIFFNESS MATRIX $K_o$

This matrix represents the exact linear case with two limitations: the loads must be applied at the node points of the structure and the section properties between nodes must remain constant.

A structure matrix was generated by standard methods and the results for various load cases were compared to existing theoretical solutions. Two structures were analyzed, a cantilever and a restrained beam. The cantilever had all degrees of freedom fixed at one end, and all free at the other. The restrained beam had all degrees of freedom fixed at one end, but only the flange rotations were fixed at the other end. This allowed placing an end torque on the restrained beam. The results are given in Fig. 6.

From Fig. 6 it can be seen that the matrix gives the same results as the strength of materials solution. This is to be expected since no approximation to the strength of material solution was used in the derivation.

In some beams, most of the torque can be carried in pure torsion. If the beam is represented with many short elements which tend to carry most of the torsion in flange bending, the question arises as to whether the matrices contain sufficient accuracy to convert the weak pure torsion resistance of the element to the predominant pure torsion resistance of the main structure. In other words, if there is insufficient accuracy in the computation procedure, the flange shear may overshadow the pure torsion terms in short elements and produce erroneous results when summed into a large structure.

In order to investigate this problem several structures of varying length were analyzed. Each structure was fully restrained at one end, and had the flange rotations restrained at the other end. For each of these structures, a plot of torque carried by shear over total torque (Vh/T) against x was made, where the results came from strength of materials calculations.

The results are given in Fig. 7.

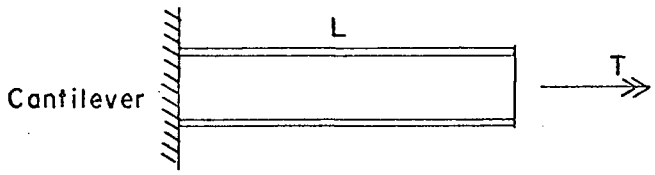


$I = 41.6\ in^4$ $E = 30000\ k/in^2$

$J = 1.25\ in^4$ $G = 10000\ k/in^2$

$h = 10"$

L = 240" @ 3 Segments

| x | Strength of Material Flange Moment (Kip inches) | Matrix Value Flange Moment (Kip inches) | Strength of Material Flange Deflections (inches) | Matrix Value Flange Deflections (inches) |
|---|---|---|---|---|
| 0 | 70.5 | 70.496 | 0. | 0. |
| 80" | 22.32 | 22.501 | 0.1270 | 0.128 |
| 160" | 6.55 | 6.57 | 0.3850 | 0.3843 |
| 240" | 0. | 0. | 0.678 | 0.6780 |

L = 240" @ 1 Segment

| | | | | |
|---|---|---|---|---|
| 0 | 70.5 | 70.496 | 0. | 0. |
| 240" | 0. | 0. | .678 | 0.6780 |

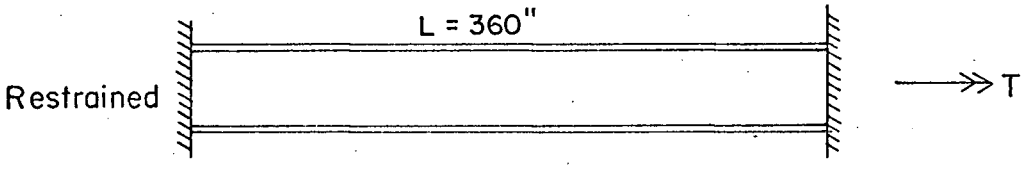


Properties as above

| x | 10 Segments @ 36" | | 15 Segments @ 24" | |
|---|---|---|---|---|
| | Strength of Material Flange Moment (Kip inches) | Matrix Value Flange Moment (Kip inches) | Strength of Material Flange Moment (Kip inches) | Matrix Value Flange Moment (Kip inches) |
| 0 | 69.8 | 69.795 | 69.8 | 69.807 |
| 36" | 41.5 | 41.473 | - | - |
| 72" | 24.15 | 24.155 | 24.15 | 24.161 |
| 108" | 13.26 | 13.244 | - | - |
| 144" | 5.86 | 5.846 | 5.86 | 5.87 |
| 180" | 0. | 0. | - | - |

Fig. 6 TEST RESULTS FOR $K_o$

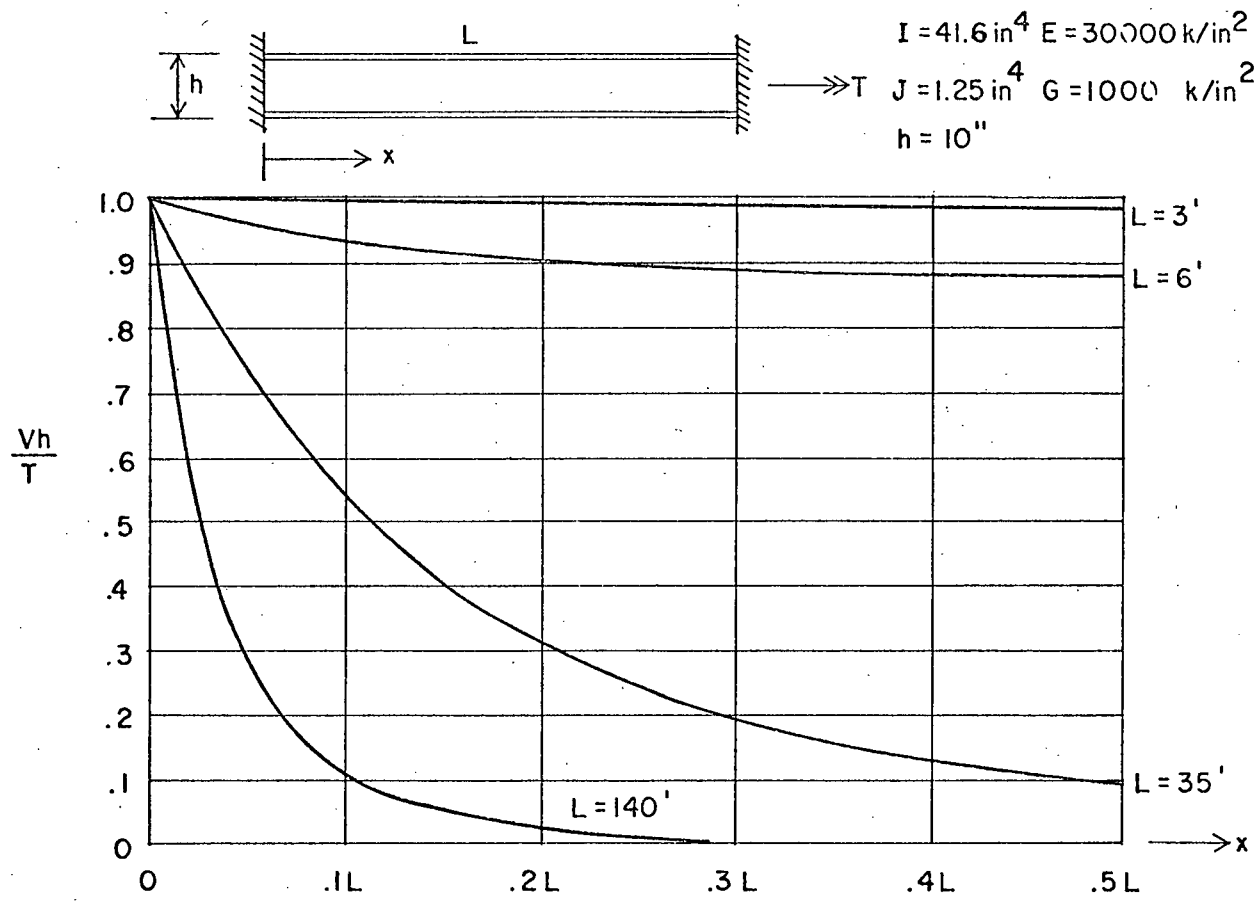


Fig. 7 EFFECT OF FLANGE WARPING

It can be seen from Fig. 7 that the effects of the flanges in carrying torsion for members of this type is considerable and in the case of short members, the flanges carry virtually the entire torque. This would indicate that caution should be exercised in representing structures with a large number of elements. However, a thirty foot beam of the same type as represented in Fig. 7 was analyzed accurately using two foot elements (see Fig. 6) so the problem is not overly serious.

The linear matrix developed in this section, or variation on it, should be used in the analysis of grid frameworks composed of wide flange sections, as it considers the effect of flange warping. This is important, as flange warping may account for a large part of the torsional strength of a wide flange section.

# CHAPTER III

## DEVELOPMENT OF NON-LINEAR DIFFERENTIAL EQUATIONS

The beam element may be subjected to moments, shears and axial loads in the major principal axes as shown in Fig. 8.

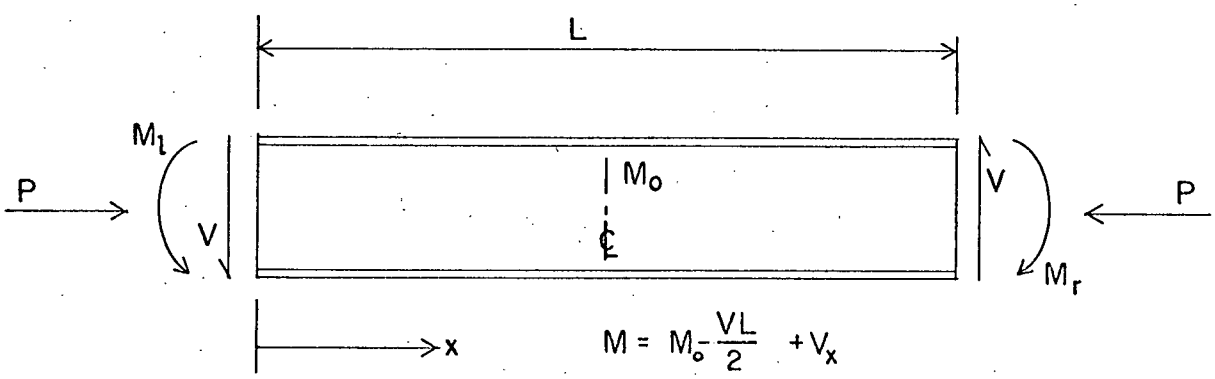


Fig. 8 SIGN CONVENTION FOR PRINCIPAL SHEAR, MOMENT AND AXIAL LOAD

When this condition exists, the element behaviour is no longer linear, and a structure composed of these elements may reach a condition of instability. To investigate this condition, elements of the web and flange under the action of P, M, and V were examined in a displaced position, as shown in Fig. 9.

From symmetry, the shear center of the section coincides with the centroid, and its lateral deflection is measured by y, as shown in Fig. 9(a). Lateral deflections of points other than the centroid are found from the relation $y_1 = y + \phi\eta$. Due to the presence of P, M and V, the differential elements are under the action of stresses $\sigma$ and $\tau$ as shown in Figs. 9(b), (c), (d), (e) where

$$\sigma = \left(\frac{P}{A} - \frac{M\eta}{I_y}\right) = \sigma_o - \frac{M\eta}{I_y} \qquad \text{and} \qquad \tau = \frac{V}{A_w}$$

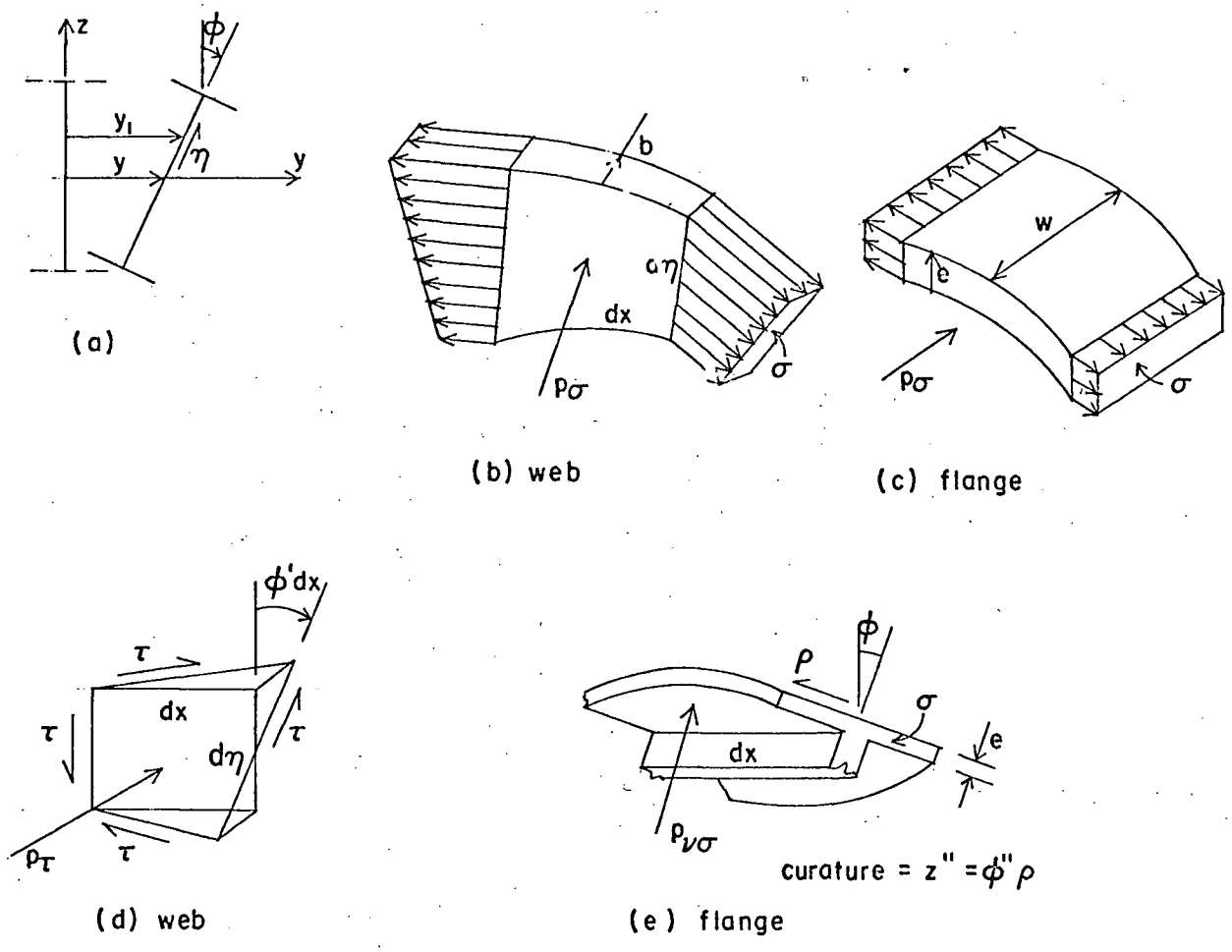


Fig. 9 ELEMENTAL BEAM SECTIONS IN DISPLACED POSITION UNDER THE ACTION OF PRIMARY STRESSES

The shear stress $\tau$ is assumed constant over the web and the bending moment M is given by

$$M = M_o - \frac{VL}{2} + Vx$$

The stresses $\sigma$ and $\tau$ may be considered as generating lateral pressures in the y direction of $p_\sigma$ and $p_\tau$, as shown in Figs. 9(b), (c), (d), which act on the element where

$$p_\sigma = \left(\sigma_o - \frac{M\eta}{I_y}\right) y_1'' \, t = \left(\sigma_o - \frac{M\eta}{I_y}\right) (y'' + \phi'' \eta) \, t \qquad (8)$$

$$p_\tau = \tau t \phi' + 2\tau t \frac{\phi'}{2} = 2\tau \phi' t \qquad (9)$$

where $t = b$ in the web

$= w$ in the flange

The stresses $\sigma$ may also be thought of as generating vertical pressures acting on elements in the top flange of value $p_{v\sigma}$, as shown in Fig. 9(e), where

$$p_{v\sigma} = \left(\sigma_o - \frac{Mh}{2I_y}\right) \phi'' \rho e \tag{10}$$

By integrating these pressures over their respective areas and dividing by dx, the forces and torques per unit length can be obtained. They are given by

$$\text{Lateral force/Length} = \frac{1}{dx} \int_{\eta=-h/2}^{+h/2} (p_\sigma + p_\tau)\, d\eta\, dx \tag{11}$$

$$\text{Torque/Length} = \frac{1}{dx} \int_{\eta=-h/2}^{+h/2} (p_\sigma + p_\tau)\, \eta d\eta\, dx + \frac{1}{dx} \int_{\rho=-w/2}^{+w/2} p_{v\sigma}\, \rho d\rho\, dx \tag{12}$$

$$\text{Vertical force/Length} = \frac{1}{dx} \int_{\rho=-w/2}^{+w/2} p_{v\sigma}\, d\rho \tag{13}$$

Now, the lateral force/unit length becomes the R.H.S. of eq.(4) to give:

$$2EIy'''' = \int_{\eta=-h/2}^{+h/2} \left[-\left(\sigma_o - \frac{M\eta}{I_y}\right)(y'' + \phi''\eta)\, t + 2\tau\phi' t\right] d\eta \tag{14}$$

The torque/unit length becomes the R.H.S. of eq.(3) to give:

$$\frac{EIh^2}{2}\phi'''' - C\phi'' = \int_{\eta=-h/2}^{+h/2} \left[-\left(\sigma_o - \frac{M\eta}{I_y}\right)(y'' + \phi''\eta)\, \eta t + 2\tau\phi' t\eta\right] d\eta$$

$$+ \int_{\rho=-w/2}^{+w/2} -\left(\sigma_o - \frac{M\eta}{2I_y}\right) \phi'' \rho^2 e d\rho + \int_{\rho=-w/2}^{+w/2} -\left(\sigma_o + \frac{M\eta}{2I_y}\right) \phi'' \rho^2 e d\rho \tag{15}$$

The vertical force/unit length affects the z deflection of the centroid of the section in the following manner:

$$EI_y z'''' = \int_{\rho=-w/2}^{+w/2} \left(\sigma_o - \frac{Mh}{2I_y}\right) \phi'' \rho e d\rho + \int_{\rho=-w/2}^{+w/2} \left(\sigma_o + \frac{Mh}{2I_y}\right) \phi'' \rho e d\rho \tag{16}$$

By multiplying out, integrating, and using the symmetry properties of the section, eqs. (14), (15), (16) reduce to the governing differential equation of the section as follows:

$$2EIy'''' = -Py'' + M\phi'' + 2\phi V' \tag{17}$$

$$\frac{EIh^2\phi''''}{2} - C\phi'' = -\sigma_o I_p \phi'' + My'' \tag{18}$$

$$EI_y z'''' = 0 \tag{19}$$

where $I_p$ = polar moment of inertia about centroid.

Equation (19) is the equation governing the vertical deflections of the section. It states that the principal axes forces M, P and V have no effect on the vertical deflections when the element undergoes a lateral or torsional displacement. It should be noted though that there will be some effect on the y, z and $\phi$ deflections due to vertical deflection, but in this derivation the vertical deflections are assumed to be small and their effect is taken as zero.

The exact solution for the differential equations for the various end conditions required by the stiffness matrix would be difficult to obtain. Instead an iterative technique will be developed.

If the beam is represented by several elements, these will be much shorter than the structure. This means the deflections of the element relative to its local co-ordinates will be much smaller than the structure deflections and consequently the element will be much stiffer than the structure. Because of this, the critical P, M and V for the structure will be much lower than the

critical P, M and V for the element. Thus the P, M and V in each element will have only a small effect in modifying the deflections; consequently the linear shape, previously obtained, will be quite close to the final deflected shape.

By placing the linear deflections, which were previously obtained, into the R.H.S. of eqs.(17) and (18) we obtain new linear equations, in which the effect of M, P and V will be approximately accounted for; solving these new equations for homogeneous boundary conditions yields increments in y and $\phi$.

This process can be repeated using the newly obtained y and $\phi$ to get a further refinement on the linear y and $\phi$.

This may be simply written as

$$2EIy''''_{n+1} = - Py''_n + M\phi''_n + 2V\phi'_n \tag{20}$$

$$\frac{EIh^2}{2}\phi''''_{n+1} - C\phi''_{n+1} = - \sigma_o I_p \phi''_n + My''_n \tag{21}$$

where n = 0, 1, 2 ... and $y_o$ and $\phi_o$ represent the linear deflections.

Since the boundary conditions are satisfied by the linear deflections $y_o$ and $\phi_o$, the sequence of new solutions $y_n$ and $\phi_n$, n = 1, 2 ... as remarked above must satisfy homogeneous boundary conditions.

Upon termination of the iteration procedure, the final results may be obtained by summing the $y_n$ and $\phi_n$ functions obtained, as shown in eqs.(22)

$$\begin{aligned} y &= y_o + y_1 + y_2 \ldots \ y_n \\ \phi &= \phi_o + \phi_1 + \phi_2 \ldots \ \phi_n \end{aligned} \tag{22}$$

By using this technique, the final y and $\phi$ obtained satisfy the required end conditions, and the terms in the stiffness matrix can be found by suitable differentiation of y and $\phi$.

As has been previously indicated, the use of several elements to represent a structure reduces the effect of M, P and V on the element deflections. Indeed, this effect can be made as small as we please by taking

sufficient elements; in these circumstances, then, it can be maintained that one iteration of eqs. (20) and (21) will give sufficient accuracy in the results. Since the linear forces have already been found from $y_o$ and $\phi_o$, it only remains to find the forces due to $y_1$ and $\phi_1$. These forces will be the non-linear terms of interest, and the matrix obtained from them will be called $K_1$. This matrix may be thought of arising from a known distributed load, due to a previously obtained set of y and $\phi$, being applied to the linear differential equations.

It should be noted that the use of $y'''$ and $y''$ to find shears and moments implies that the co-ordinate system in which the forces on the beam are represented translates and rotates with the member. In other words, the forces are tangent and perpendicular to the final deflected beam shape. This means that the forces on the beam end must be transferred into the structure co-ordinate system. Since the forces found from the differential equation need only be modified by the cosine of angles $\phi$ or $y'$, they remain basically unchanged for small deflection theory. However, since the principal forces M, P and V are also represented in these axes, they must also be transformed into structure co-ordinates by the use of the sine of $\phi$ or $y'$. Since for small deflection theory sine $\theta = \theta$, the components will be the forces of interest multiplied by the deflection of interest. The joint forces must be suitably adjusted to account for the presence of these components. These component forces may be thought of as point loads, and the matrix due to their effects will be called $K_2$. Since these forces are due only to the linear end deflections of the element, they are unaffected by element length or assumed end conditions for the solution of the non-linear differential equations.

For convenience of reference, the effective distributed loads will be known as loads of the first type and the point loads will be known as loads of the second type. The complete non-linear portion of the matrix is then

$K_1 + K_2$, to which must be added the linear matrix $K_o$.

Although the numerical technique as described simplifies the solution of the differential equations, it still entails the solution of a second order differential equation as well as several integrations. It is therefore proposed to overcome this work with a further approximation or simplification to be described in the next chapter.

# CHAPTER IV

## METHODS OF APPROXIMATIONS

Before presenting the next approximation used in the solution of the differential equation, it may prove valuable to investigate this same approximation applied to a simpler and more familiar problem.

In the analysis of beams under the action of distributed loads, one method of treatment entails dividing the beam into several segments by introducing new joints along the member as in Fig. 10(a).

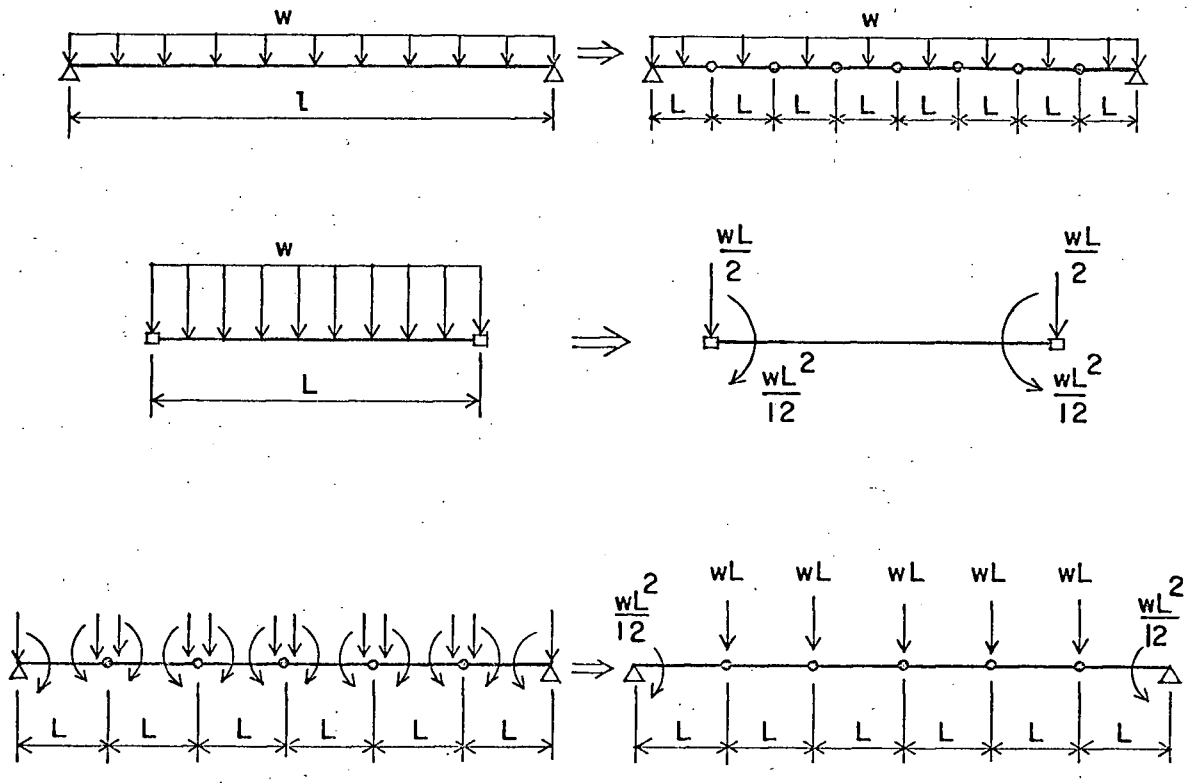


Fig. 10 REPLACING DISTRIBUTED LOADS BY FIXED END REACTIONS

The distributed load on each segment is then replaced by fixed end reactions acting at the joints, as in Fig. 10(b). When these are placed on the beam as joint loads, the moments cancel at the interior joints and are present only at the end joints, as in Fig. 10(c). These are usually ignored as they have negligible effect on the analysis results if sufficient elements are used.

For beams with an arbitrary load distribution, the end moments will not in general cancel at each interior joint. However, the end shears are proportional to the length of the element, whereas the end moments are proportional to the length squared. This means that as the length L goes to zero, the end moments decrease faster than the end shears. Therefore, by decreasing L, which means increasing the number of elements, the moments approach zero. Since an increase in the number of elements also causes the distributed loads on adjacent members to approach each other in value, the end moments not only approach zero, they approach each other but with a sign difference. A good approximation is then obtained by using several elements, ignoring the small moment resultants, and using only the end shears. This amounts to replacing the fixed end reactions of each element by pin-end reactions.

This leads to the next approximation in the solution of the differential equation for lateral torsional buckling:

Apply the type one loads of the R.H.S. of eqs.(20) and (21) to a simply supported element rather than a fixed element.

This will eliminate end moments acting at the joints due to loads of type one. The type two loads exist unchanged by this approximation.

# CHAPTER V

## ILLUSTRATION OF METHODS OF APPROXIMATIONS

As an illustration of the above method and approximation, the buckling matrix of a beam column will be developed with the type one loads acting on a fixed element and then on a simply supported element. Each non-linear matrix will be developed in two parts: a first part due to type one loads and a second part due to type two loads. The exact matrix is given by Gere and Weaver [2].

For a beam element under constant axial load, the differential equation is

$$EIy'''' = - Py'' \tag{23}$$

for the element of Fig. 11(a). Equation (23) will be applied to a fixed ended element first, utilizing the sign convention of Fig. 1(b) for shear, moment and load.

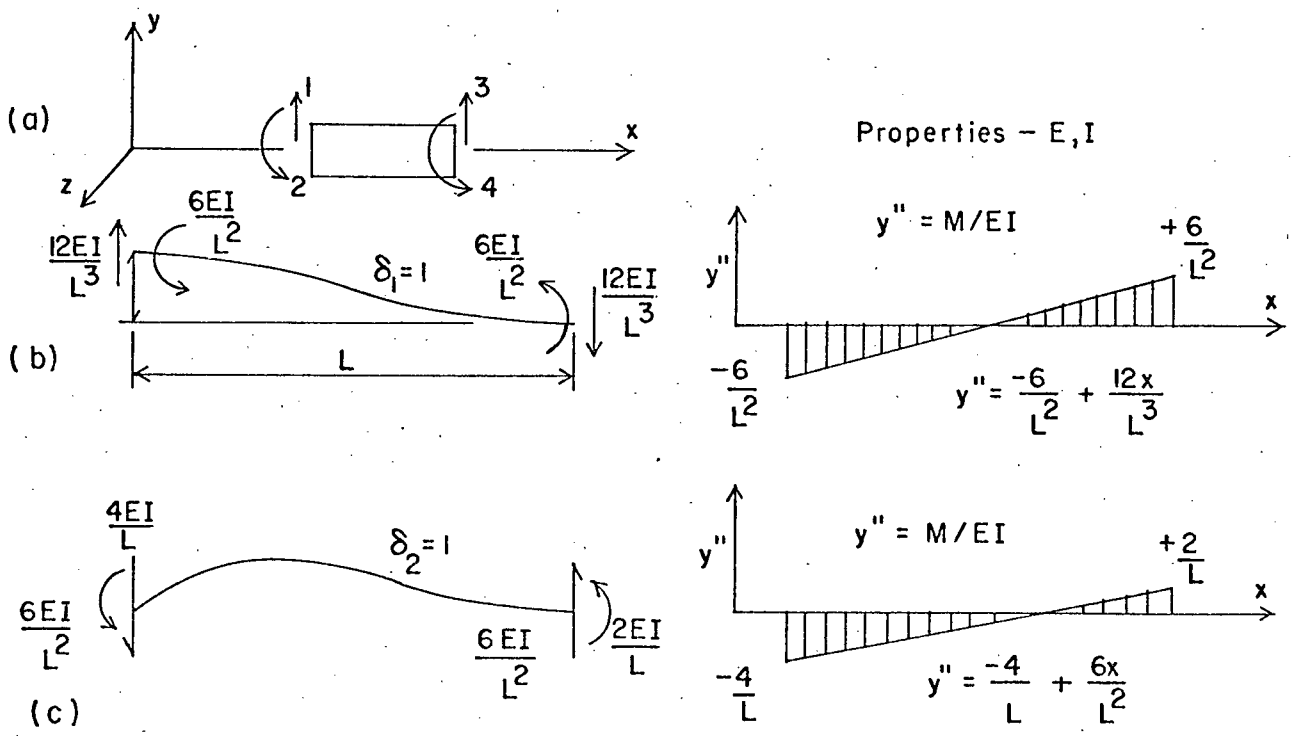


Fig.11 ORDINARY BEAM STIFFNESS DEFLECTIONS, FORCES AND CURVATURES

The equation of $y_o''$ for $\delta_1$ equals unity is

$$y_o'' = -\frac{6}{L^2} + \frac{12x}{L^3} \tag{24}$$

Substitution of eq.(24) into the R.H.S. of eq. (23) gives

$$EIy_1'''' = -P\left[\frac{-6}{L^2} + \frac{12x}{L^3}\right] \tag{25}$$

Integration gives

$$EIy_1''' = -P\left[\frac{-6x}{L^2} + \frac{6x^2}{L^3} + A\right] \tag{26}$$

$$EIy_1'' = -P\left[-\frac{3x^2}{L^2} + \frac{2x^3}{L^3} + Ax + B\right] \tag{27}$$

$$EIy_1' = -P\left[-\frac{x^3}{L^2} + \frac{x^4}{2L^3} + \frac{Ax^2}{2} + Bx + C\right] \tag{28}$$

$$EIy_1 = -P\left[-\frac{x^4}{4L^2} + \frac{x^5}{10L^3} + \frac{Ax^3}{6} + \frac{Bx^2}{2} + Cx + D\right] \tag{29}$$

It is to be remembered that the $y_1$ in the above equation is the $y_1$ due to loads of type one.

For a fixed element, the end conditions are:

@x = 0 $\quad y_1 = 0 \quad y_1' = 0$ @x = L $\quad y_1 = 0 \quad y_1' = 0$

Using these end conditions and solving for the constants gives

A = 6/5L

B = - 1/10

C = 0

D = 0

Eqs.(26) and (27) then give end shears and moments as

$$@x = 0 \quad M = EIy_1'' = P/10 \qquad @x = L \quad M = EIy_1'' = -P/10$$

$$V = EIy_1''' = -6P/5L \qquad V = EIy_1''' = -6P/5L$$

$$\text{For } \delta_2 = 1,\ y_0'' = -\frac{4}{L} + \frac{6x}{L^2} \tag{30}$$

Substitution of eqs.(30) into eqs.(23) gives

$$EIy_1'''' = -P\left(-\frac{4}{L} + \frac{6x}{L^2}\right) \tag{31}$$

Integration gives

$$EIy_1''' = -P\left(-\frac{4x}{L} + \frac{3x^2}{L^2} + A_1\right) \tag{32}$$

$$EIy_1'' = -P\left(-\frac{2x^2}{L} + \frac{x^3}{L^2} + A_1x + B_1\right) \tag{33}$$

$$EIy_1' = -P\left(-\frac{2x^3}{3L} + \frac{x^4}{4L^2} + A_1\frac{x^2}{L} + B_1x + C_1\right) \tag{34}$$

$$EIy_1 = -P\left(-\frac{2x^4}{12L} + \frac{x^5}{20L^2} + \frac{A_1x^3}{6} + \frac{B_1x^2}{2} + C_1x + D_1\right) \tag{35}$$

The end conditions for a fixed element are

$$@x = 0 \quad y_1 = 0 \qquad x = L \quad y_1 = 0$$

$$y_1' = 0 \qquad y_1' = 0$$

Solving for the constants yields

$A_1 = 11/10$

$B_1 = -2L/15$

$C_1 = 0$

$D_1 = 0$

Substitution of $A_1$, $B_1$, $C_1$ and $D_1$ into eqs.(32) and (33) yields the shears and moments of interest.

@x = 0 $\quad M = EIy_1'' = 2PL/15$ $\qquad$ @x = L $\quad M = EIy_1'' = PL/30$

$\qquad V = EIy_1''' = -11P/10$ $\qquad\qquad V = EIy_1''' = -P/10$

The end forces for $\delta_3$ and $\delta_4$ equal to one can be found using similar calculations to the ones above. When the results are placed in matrix form, they give the portion of the non-linear matrix due to loads of the first type acting on a fixed ended element. The matrix is given in Fig. 12.

| | | | |
|---|---|---|---|
| $-\frac{6P}{5L}$ | $-\frac{11P}{10}$ | $+\frac{6P}{5L}$ | $-\frac{P}{10}$ |
| $-\frac{P}{10}$ | $-\frac{2PL}{15}$ | $+\frac{P}{10}$ | $+\frac{PL}{30}$ |
| $+\frac{6P}{5L}$ | $+\frac{P}{10}$ | $-\frac{6P}{5L}$ | $+\frac{11P}{10}$ |
| $-\frac{P}{10}$ | $+\frac{PL}{30}$ | $+\frac{P}{10}$ | $-\frac{2PL}{15}$ |

Fig. 12 NON-LINEAR BEAM COLUMN MATRIX FOR TYPE 1 LOADS, FIXED END CONDITIONS

For the portion of the non-linear matrix due to loads of the second type, the value of the linear end displacement need be considered. See Fig.13.

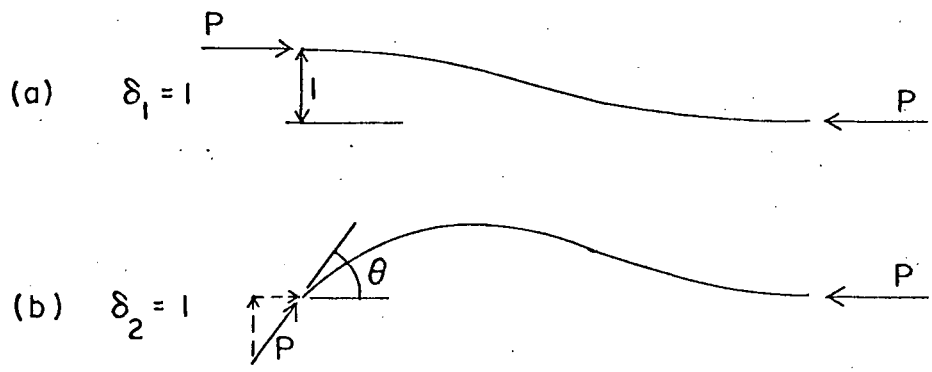


Fig. 13 NON-LINEAR BEAM COLUMN TERMS FOR TYPE 2 LOADS

For $\delta_1 = 1$, as in Fig. 13(a), there are no components of P acting in the shear direction, so there are no contributions in the second portion of the matrix for this deflected shape.

For $\delta_2 = 1$, as in Fig. 13(b), the load P which the joint must provide has a component in the shear direction of value P × sine ($\theta$) = P$\theta$ = P at the L.H.S of the structure. This value must be entered in the shear force position of the matrix for $\delta_2 = 1$. The R.H.S has no component.

By treating the other deflections the same way, the second portion of the non-linear matrix is built up as shown in Fig. 14.

| | | | |
|---|---|---|---|
| 0 | +P | 0 | 0 |
| 0 | 0 | 0 | 0 |
| 0 | 0 | 0 | -P |
| 0 | 0 | 0 | 0 |

Fig. 14 NON-LINEAR BEAM COLUMN MATRIX FOR TYPE 2 LOADS

When the matrices presented in Figs. 12 and 14 are added, the result is the complete second order matrix as shown in Fig. 15.

| | | | |
|---|---|---|---|
| $-\frac{6P}{5L}$ | $-\frac{P}{10}$ | $+\frac{6P}{5L}$ | $-\frac{P}{10}$ |
| $-\frac{P}{10}$ | $-\frac{2PL}{15}$ | $+\frac{P}{10}$ | $+\frac{P}{30}$ |
| $+\frac{6P}{5L}$ | $+\frac{P}{10}$ | $-\frac{6P}{5L}$ | $+\frac{P}{10}$ |
| $-\frac{P}{10}$ | $+\frac{PL}{30}$ | $+\frac{P}{10}$ | $-\frac{2PL}{15}$ |

Fig. 15 COMPLETE NON-LINEAR BEAM COLUMN MATRIX, FIXED END CONDITIONS

In summary, this matrix was found by using the linear deflected shape to generate a load to use in eq.(23). This load was applied to an element fixed at the ends.

It is of interest to note at this point the relation between the exact matrix for buckling, containing sine and cosine functions, and the approximate matrix in Fig. 16. If the series expansions for the sine and cosine are substituted into the exact matrix, the second term of this expansion gives the approximate matrix derived above.

Equation (23) will now be applied to a pin ended element.

Fig. 12 still represents the linear deflected shapes and the type one loads. To solve for the forces, it is only necessary to integrate eq.(23) twice since the known end conditions of $y_1'' = 0$ at the ends will solve the two constants of integration, and then one differentiation will give the end shears. However, because of the simple type one loads for these cases, statics can be used to determine the end shears, as in Fig. 16.

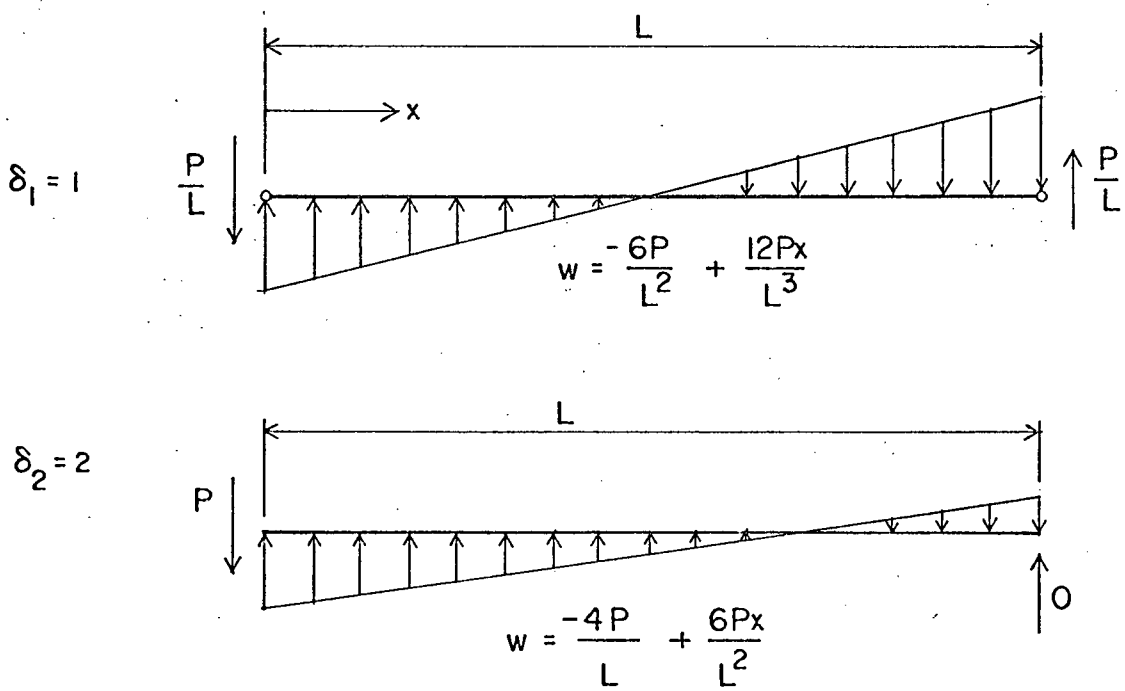


Fig. 16 NON-LINEAR BEAM COLUMN TERMS FOR TYPE 1 LOADS, PINNED END CONDITIONS

Similarly, the end forces for $\delta_3$ and $\delta_4$ equal to one can be obtained. Combining the end forces into matrix form gives the portion of the non-linear matrix due to loads of the first type acting on a pinned element. See Fig. 17.

| | | | |
|---|---|---|---|
| $-\frac{P}{L}$ | $-P$ | $-\frac{P}{L}$ | 0 |
| 0 | 0 | 0 | 0 |
| $+\frac{P}{L}$ | 0 | $-\frac{P}{L}$ | $+P$ |
| 0 | 0 | 0 | 0 |

Fig. 17 NON-LINEAR BEAM COLUMN MATRIX FOR TYPE 1 LOADS, PINNED END CONDITIONS

The portion of the matrix due to loads of the second type remains unchanged. Therefore, the complete matrix is found by adding the matrix of Fig.17 and Fig. 14. This yields a relatively simple matrix, as shown in Fig. 18.

| | | | |
|---|---|---|---|
| $-\frac{P}{L}$ | 0 | $+\frac{P}{L}$ | 0 |
| 0 | 0 | 0 | 0 |
| $+\frac{P}{L}$ | 0 | $-\frac{P}{L}$ | 0 |
| 0 | 0 | 0 | 0 |

Fig. 18 COMPLETE NON-LINEAR BEAM COLUMN MATRIX, PINNED END CONDITIONS.

It is of interest to note that this is the non-linear matrix for a pin-ended strut under axial load.

The effect of the approximations will now be considered. Three structures, a pinned column, a fixed column with a pin at the center and a fixed column were analyzed using the matrices presented in Fig. 18 and Fig. 15. Each column was analyzed using a varying number of elements. The per cent errors in the results of each analysis were plotted against the number of elements used for each column, as shown in Fig. 19.

It should be noted that the forces due to loads of the second type in the matrix are of no importance in members with continuous deflections. This arises from the fact that the adjoining ends of elements in a continuous structure have the same deflections but the end forces are of opposite sign. The contributions of end forces to each joint from each member then cancel each other out. However, if a pin exists in the structure, continuity of slope no longer exists and the end force components of adjacent elements may not be self cancelling. This implies that the type one loads are all that is necessary to analyze continuous structures, but that they will fail to analyze structures with interior pins. The results of analysis of various interior pinned column using matrices with and without the effects of loads of the second type bear this out.

In conclusion then, it is proposed to calculate $y_1$ on the basis of $y_1 = y_1'' = 0$ at each end and just use the calculated end shears in the matrix rather than using $y_1 = y_1' = 0$ as the end conditions and using the associated calculated shears and moments in the matrix. The type two terms, which are added to the above results, are the same for either set of assumed end conditions.

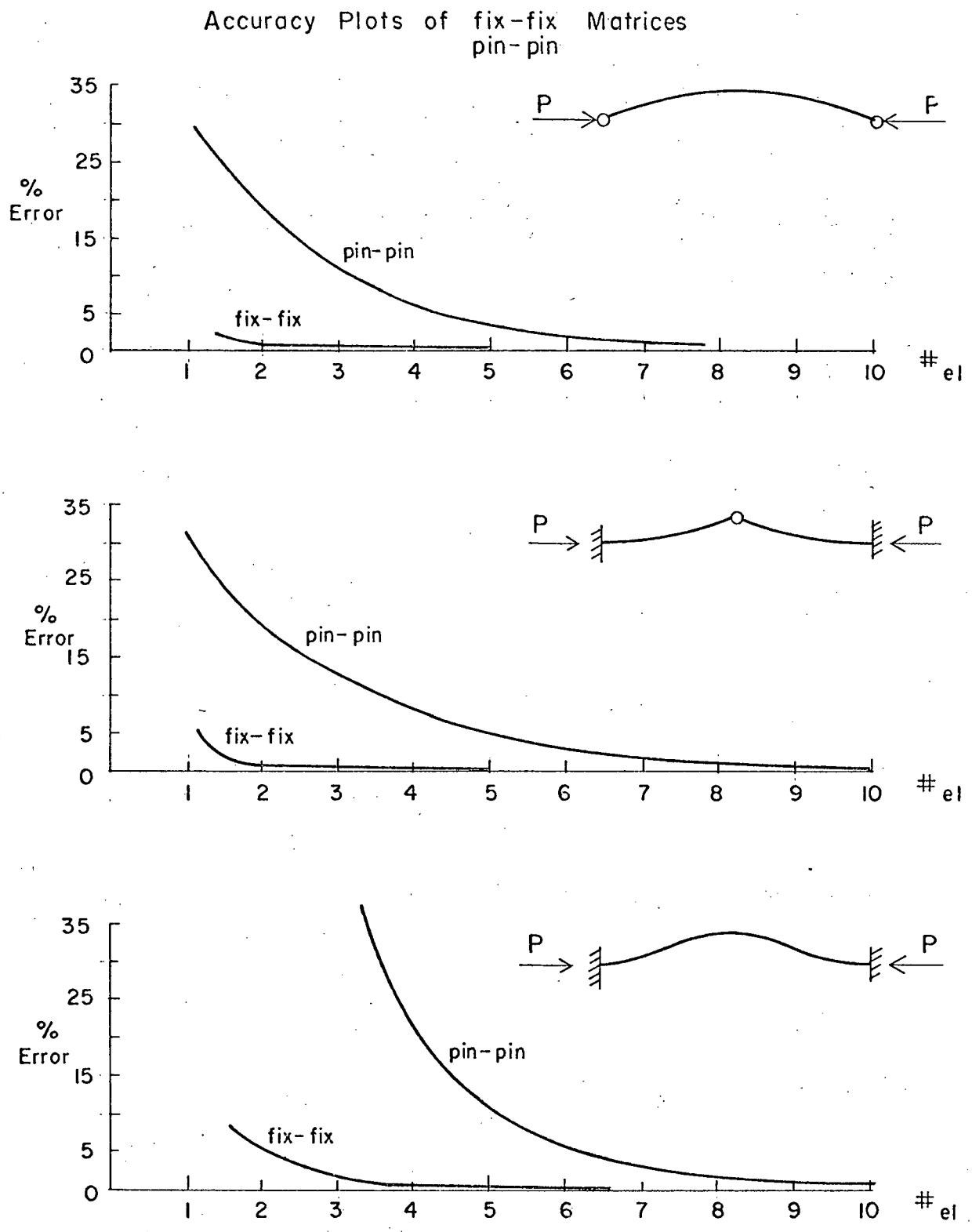


Fig. 19 PLOT OF % ERROR VS. NO. OF ELEMENTS FOR BEAM-COLUMN MATRICES FOR 3 COLUMN TYPES

# CHAPTER VI

## DEVELOPMENT OF LATERAL STABILITY MATRIX

### i Application of Approximations

Only one iteration will be used to develop the matrix. The linear portion of the matrix, corresponding to the deflections $y_o$ and $\phi_o$, has already been obtained. The non-linear terms of the matrix due to $y_1$ and $\phi_1$ will now be found by solving the differential equation for $y_1$ and $\phi_1$ using boundary conditions of $y_1 = y_1'' = \phi_1 = \phi_1'' = 0$ at each end. Shears and torques are then found from $y_1$ and $\phi_1$. It is deduced from the previous section that it is not necessary to use $y_1 = y_1' = 0$ and $\phi_1 = \phi_1' = 0$ at each end as boundary conditions. Once again, the type two load terms are independent of whichever boundary conditions are used. However, the use of statics to determine the end shears on a pinned element was discarded as the type one loads were more complex than those associated with the beam column. Instead, the governing differential equations, after substitution of the linear deflections in the R.H.S were integrated twice and then solved for the end conditions.

Equations (20) and (21) become for n = 0,

$$2EIy_1'''' = - Py_o'' + M\phi_o + 2V\phi_o'' \tag{36}$$

$$\frac{EIh^2}{2}\phi_1'''' - C\phi_1'' = - \sigma_o I_p \phi_o'' + My_o'' \tag{37}$$

Integrating twice, eqs.(36) and (37) become

$$2EIy_1'' = - Py_o + \int\int M\phi_o'' \, dxdx + 2V\int \phi_o dx + Ax + B \tag{38}$$

$$\frac{EIh^2}{2}\phi_1'' - C\phi_1 = - \sigma_o I_p \phi_o + \int\int My_o'' \, dxdx + Dx + E \tag{39}$$

Integrating $\int\int M\phi_o''\,dxdx$ by parts, and remembering $M' = V$ and $V' = 0$, gives

$$\int\int M\phi_o''\,dxdx = \int M\phi_o'\,dx - \int \phi_o V dx \tag{40}$$

Integration of $\int M\phi_o' dx$ by parts gives

$$\int M\phi_o' dx = M\phi_o - V\int \phi_o dx \tag{41}$$

Substitution of (41) into (40) gives

$$\int\int M\phi_o''\,dxdx = M\phi_o - 2V\int \phi_o dx \tag{42}$$

A similar integration gives

$$\int\int My_o''\,dxdx = My_o - 2V\int y_o dx \tag{43}$$

Now, substitution of eqs.(43) and (42) into eqs.(38) and (39) gives

$$2EIy_1'' = - Py_o + M\phi_o + Ax + B \tag{44}$$

$$\frac{EIh^2}{2}\phi_1'' - C\phi_1 = - \sigma_o I_p \phi_o + My_o - 2V\int y_o dx + Ex + D \tag{45}$$

The end conditions of $\phi_1 = \phi_1'' = y_1 = y_1'' = 0$ were then applied to equations (44) and (45). These equations lend themselves to this approach, as the L.H.S of both equations become zero at x = 0, L, and the R.H.S of the equations contains only the values of the linear deflections at x = 0, L, the integration of $y_o$, and four unknown constants. These constants A, B, C, D are easily found and the non-linear matrix forces due to loads of type one are then obtained by application of the differential equations (46).

$$\begin{aligned} \text{Shear} &= EIy_1''' = - Py_o' + M\phi_o' + V\phi_o + A \\ \text{Torque} &= C\phi_1' - \frac{EIh^2}{2}\phi_1''' = + \sigma_o I_p \phi_o' - My_o' + Vy_o - E \end{aligned} \tag{46}$$

ii Calculation of Non-linear Stiffness Matrix for Type One Loads

The terms of the non-linear matrix will be calculated first for $\delta_7 = 1$, for which $y_o''$ is given by one half of Fig. 3(a) or,

$$y_o'' = \frac{3}{L^2} - \frac{6x}{L^3} \tag{47}$$

Integrating eq.(47) three times gives

$$\int y_o dx = \frac{x^3}{2L^2} - \frac{x^4}{4L^3} \tag{48}$$

A constant should be added to eq.(48), but it is taken to be combined with D in eq.(45). From Fig. 4, the values of the linear deflections at the ends of the element for $\delta_7 = 1$ are:

$$\begin{array}{llll} x = 0 & y_o = 0 & x = L & y_o = 1/2 \\ & \phi_o = 0 & & \phi_o = 1/h \\ & y_o' = 0 & & \phi_o' = 0 \\ & \phi_o' = 0 & & y_o' = 0 \end{array} \tag{49}$$

The end conditions for solution of eqs. (44) and (45) are

$$y_1 = y_1'' = \phi_1'' = \phi_1 = 0 \qquad @x = 0,L \tag{50}$$

Using eqs.(50), (49) with the differential equation (44) gives

$$x = 0 \quad 2EI[0] = - P[0] + M[0] + A[0] + B \tag{51}$$

$$x = L \quad 2EI[0] = - P[1/2] + M[1/h] + A[L] + B \tag{52}$$

Solving eqs. (51) and (52) for A and B gives

$$B = 0 \qquad A = \frac{+P}{2L} - \frac{(M_o + \frac{VL}{2})}{hL}$$

Using eqs.(49) and (50) with the differential equation (45) gives

$$x = 0 \qquad \frac{EIh^2}{2}[0] - C[0] = -\sigma_o I_p[0] + M[0] - 2V[0] + E[0] + D \tag{53}$$

$$x = L \qquad \frac{EIh^2}{2}[0] - C[0] = -\sigma_o I_p[1/h] + M[1/2] - 2V[L/4] + E_1 L + D \tag{54}$$

From eqs.(53) and (54),

$$D = 0 \qquad E = \frac{\sigma_o I_p}{hL} - \frac{(M_o + \frac{VL}{2})}{2L} + \frac{V}{2}$$

Substituting the values of A, B, D, E back into eqs.(46) and using the relations in (49) gives

$$\begin{aligned}
&\text{SHEAR} \quad @x = 0 \qquad Q = -P[0] + M[0] + V[0] + A \\
&\qquad\qquad = \frac{1}{L}\left(\frac{P}{2} - \frac{(M_o + \frac{VL}{2})}{h}\right) \\
&\qquad @x = L \qquad Q = -P[0] + M[0] + V[1/h] + A \\
&\qquad\qquad = \frac{V}{h} + \frac{1}{L}\left(\frac{P}{2} - \frac{(M_o + \frac{VL}{2})}{h}\right) \\
&\text{TORQUE} \quad @x = 0 \qquad T = \sigma_o I_p[0] - M[0] + V[0[ - E \\
&\qquad\qquad = -\frac{\sigma_o I_p}{hL} + \frac{(M_o + \frac{VL}{2})}{2L} + \frac{V}{2} \\
&\qquad @x = L \qquad T = \sigma_o I_p[0] - M[0] + V[1/2] - E \\
&\qquad\qquad = -\frac{\sigma_o I_p}{hL} + \frac{(M + \frac{VL}{2})}{2L}
\end{aligned} \tag{55}$$

By using suitable signs, and the relation $Q = T/h$, the column of the stiffness matrix for $\delta_7 = 1$ was built from relations (55) and is shown in Fig. 20.

| | 7 |
|---|---|
| 1 | $0$ |
| 2 | $0$ |
| 3 | $\frac{1}{2L}\left[\frac{P}{2} - \frac{M_o + \frac{VL}{2}}{h}\right] + \frac{1}{h}\left[\frac{\sigma_o I_p}{hL} - \frac{M_o + \frac{VL}{2}}{2L} + \frac{V}{2}\right]$ |
| 4 | $\frac{1}{2L}\left[\frac{P}{2} - \frac{M_o + \frac{VL}{2}}{h}\right] - \frac{1}{h}\left[\frac{\sigma_o I_p}{hL} - \frac{M_o + \frac{VL}{2}}{2L} + \frac{V}{2}\right]$ |
| 5 | $0$ |
| 6 | $0$ |
| 7 | $-\frac{1}{2}\left[\frac{V}{h} + \frac{1}{L}\left(\frac{P}{2} - \frac{M_o + \frac{VL}{2}}{h}\right)\right] - \frac{1}{h}\left[+\frac{\sigma_o I_p}{hL} - \frac{M_o + \frac{VL}{2}}{2L}\right]$ |
| 8 | $-\frac{1}{2}\left[\frac{V}{h} + \frac{1}{L}\left(\frac{P}{2} - \frac{M_o + \frac{VL}{2}}{h}\right)\right] + \frac{1}{h}\left[+\frac{\sigma_o I_p}{hL} - \frac{M_o + \frac{VL}{2}}{2L}\right]$ |

Fig. 20 TYPE 1 TERMS FOR NON-LINEAR MATRIX FOR $\delta_7 = 1$

For $\delta_6 = 1$, $y_o''$ is given by one half of Fig. 3(b) or

$$y_o'' = -\frac{1}{L} + \frac{3x}{L^2}$$

Integrating three times gives

$$\int y_o = -\frac{x^3}{6L} + \frac{x^4}{8L^2} \tag{56}$$

From Fig. 4, the values of the linear deflection at the ends of the element for $\delta_6 = 1$ are:

| | | | |
|---|---|---|---|
| $x = 0$ | $y_o = 0$ | $x = L$ | $y_o = 0$ |
| | $y_o' = 0$ | | $y_o' = +1/2$ |
| | $\phi_o = 0$ | | $\phi_o = 0$ |
| | $\phi_o' = 0$ | | $\phi_o' = +1/h$ |

(57)

The end conditions for solution of the differential equation (44) and (45) are still

$$y_1 = y_1'' = \phi_1 = \phi_1'' = 0 \tag{58}$$

Using eqs.(57) and (58) with the differential equation (44) gives

$$x = 0 \qquad 2EI[0] = -P[0] + M[0] + A[0] + B_1 \tag{59}$$

$$x = L \qquad 2EI[0] = -P[0] + M[0] + A_1 L + B_1 \tag{60}$$

From eqs.(59) and (60), $B_1$ and $A_1$ are

$$A_1 = 0 \qquad B_1 = 0$$

Using eqs.(57) and (58) with the differential equation (45) gives

$$x = 0 \qquad \frac{EIh^2}{2}[0] - C[0] = -\sigma_o I_p[0] + M[0] - 2V[0] + E_1[0] + D_1 \tag{61}$$

$$x = L \qquad \frac{EIh^2}{2}[0] - C[0] = -\sigma_o I_p[0] + M[0] - 2V\left[\frac{L}{24}\right]^2 + E_1 L + D_1 \tag{62}$$

From eqs.(61) and (62)

$$D_1 = 0 \qquad E_1 = -VL/12$$

Substitution of the values of $A_1$, $B_1$, $C_1$, $D_1$ back into eqs.(46) and using relations (57) gives

$$\begin{aligned}
&\text{SHEAR} \quad x = 0 \qquad Q = -P[0] + M[0] + V[0] \\
&\qquad\qquad\qquad\quad = 0 \\
&\qquad\quad x = L \qquad Q = -P[1/2] + \left(M_o + \frac{VL}{2}\right)(1/h) + V[0] \\
&\qquad\qquad\qquad\quad = -\frac{P}{2} + \frac{\left(M_o + \frac{VL}{2}\right)}{h} \\
&\text{TORQUE} \quad x = 0 \qquad T = +\sigma_o I_p[0] - M[0] + V[0] - E_1 \\
&\qquad\qquad\qquad\quad = +\frac{VL}{12} \\
&\qquad\quad x = L \qquad T = +\sigma_o I_p[1/h] + \left(M_o + \frac{VL}{2}\right)[1/2] + V[0] - E_1 \\
&\qquad\qquad\qquad\quad = +\frac{\sigma_o I_p}{h} - \left(M_o + \frac{VL}{2}\right) + \frac{VL}{12}
\end{aligned} \tag{63}$$

By using the relations in (63) with suitable signs, and the relation $Q = T/h$, the column of the matrix due to type one loads for $\delta_6 = 1$ was built, as shown in Fig. 21.

Similarly, the other stiffness deflections were treated. The complete non-linear portion of the matrix due to loads of type one is $K_1$ and can be written as $K_1 = Pk_{1p} + Mk_{1m} + Vk_{1v}$, as in Fig. 22. The portion of the matrix due to loads of type two must still be calculated.

| | 6 |
|---|---|
| 1 | $0$ |
| 2 | $0$ |
| 3 | $0 + \frac{1}{h}\left[-\frac{VL}{12}\right]$ |
| 4 | $0 - \frac{1}{h}\left[-\frac{VL}{12}\right]$ |
| 5 | $0$ |
| 6 | $0$ |
| 7 | $-\frac{1}{2}\left[-\frac{P}{2} + \frac{M_o + \frac{VL}{2}}{h}\right] - \frac{1}{h}\left[-\frac{\sigma_o I_p}{h} + \frac{M_o + \frac{VL}{2}}{2} - \frac{VL}{12}\right]$ |
| 8 | $-\frac{1}{2}\left[-\frac{P}{2} + \frac{M_o + \frac{VL}{2}}{h}\right] + \frac{1}{h}\left[-\frac{\sigma_o I_p}{h} + \frac{M_o + \frac{VL}{2}}{2} - \frac{VL}{12}\right]$ |

Fig. 21 TYPE 1 TERMS FOR NON-LINEAR MATRIX FOR $\delta_6 = 1$

$K_1 =$

$Pk_{p_1} = P$

| | 1 | 2 | 3 | 4 | 5 | 6 | 7 | 8 |
|---|---|---|---|---|---|---|---|---|
| 1 | 0 | 0 | 0 | 0 | 0 | 0 | 0 | 0 |
| 2 | 0 | 0 | 0 | 0 | 0 | 0 | 0 | 0 |
| 3 | - a + b | - a - b | -(a+b)/L | (-a+b)/L | 0 | 0 | (a+b)/L | (a-b)/L |
| 4 | - a - b | - a - b | (-a+b)/L | -(a+b)/L | 0 | 0 | (a-b)/L | (a+b)/L |
| 5 | 0 | 0 | 0 | 0 | 0 | 0 | 0 | 0 |
| 6 | 0 | 0 | 0 | 0 | 0 | 0 | 0 | 0 |
| 7 | 0 | 0 | (a+b)/L | (a-b)/L | a - b | a + b | -(a+b)/L | (-a+b)/L |
| 8 | 0 | 0 | (a-b)/L | (a+b)/L | a + b | a - b | (-a+b)/L | (-a-b)/L |

$Mk_{m_1} = M(\frac{1}{hL})$

| | 1 | 2 | 3 | 4 | 5 | 6 | 7 | 8 |
|---|---|---|---|---|---|---|---|---|
| 1 | 0 | 0 | 0 | 0 | 0 | 0 | 0 | 0 |
| 2 | 0 | 0 | 0 | 0 | 0 | 0 | 0 | 0 |
| 3 | 0 | +L | +1 | 0 | 0 | 0 | -1 | 0 |
| 4 | -L | 0 | 0 | -1 | 0 | 0 | 0 | +1 |
| 5 | 0 | 0 | 0 | 0 | 0 | 0 | 0 | 0 |
| 6 | 0 | 0 | 0 | 0 | 0 | 0 | 0 | 0 |
| 7 | 0 | 0 | -1 | 0 | 0 | -L | +1 | 0 |
| 8 | 0 | 0 | 0 | +1 | +L | 0 | 0 | -1 |

$Vk_{v_1} = V(\frac{1}{12h})$

| | 1 | 2 | 3 | 4 | 5 | 6 | 7 | 8 |
|---|---|---|---|---|---|---|---|---|
| 1 | 0 | 0 | 0 | 0 | 0 | 0 | 0 | 0 |
| 2 | 0 | 0 | 0 | 0 | 0 | 0 | 0 | 0 |
| 3 | +1 | -5 | 0 | -6/L | -1 | -1 | 0 | +6/L |
| 4 | +5 | -1 | +6/L | 0 | +1 | +1 | -6/L | 0 |
| 5 | 0 | 0 | 0 | 0 | 0 | 0 | 0 | 0 |
| 6 | 0 | 0 | 0 | 0 | 0 | 0 | 0 | 0 |
| 7 | -1 | -1 | 0 | -6/1 | +1 | -5 | 0 | +6/L |
| 8 | +1 | +1 | +6/L | 0 | +5 | -1 | -6/L | 0 |

$a = 1/4 \quad b = I_p/Ah^2$

Fig. 22 NON-LINEAR MATRIX FOR TYPE 1 LOADS

iii Calculation of Non-linear Matrix for Type Two Loads

The effect of the type two loads can best be calculated by splitting each stiffness deflection into its lateral and torsional component.

For $\delta_7 = 1$, the component linear deflections are given in Fig. 23.

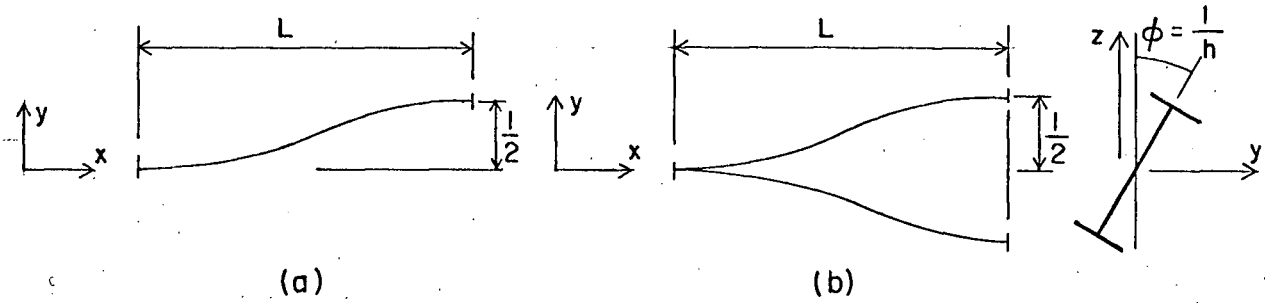


Fig. 23 COMPONENT DEFLECTIONS FOR $\delta_7 = 1$

By applying M, P and V and taking their components about the R.H.S. of the section as shown in Fig. 24, gives

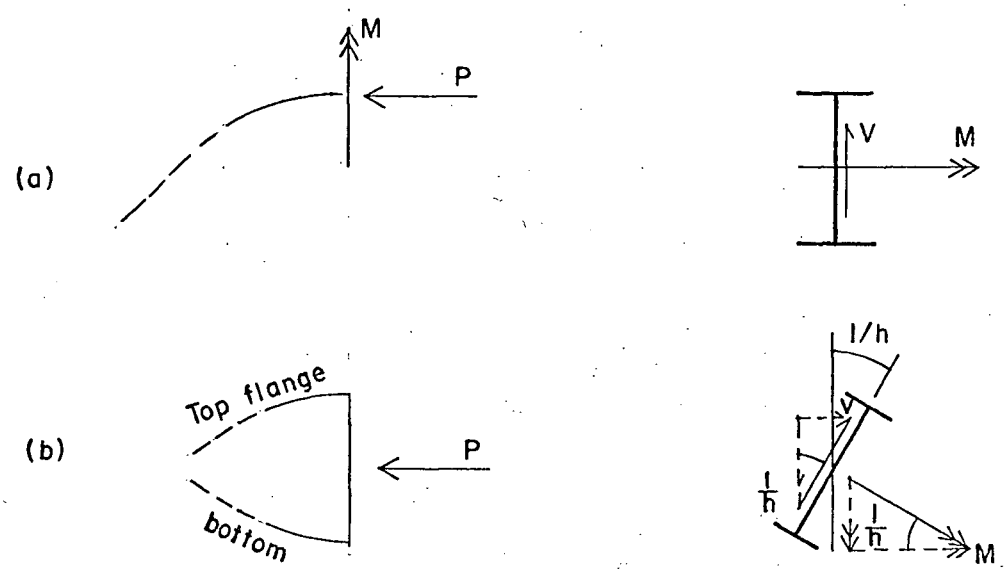


Fig. 24 FORCE COMPONENTS DUE TO END DEFLECTIONS FOR $\delta_7 = 1$

In Fig. 24(a), there are no components acting in any of the allowable joint deflections. Therefore:

$$\text{Shear} = 0$$

$$\text{Moment} = 0$$

$$\text{Torque} = 0$$

For Fig. 24(b), the components acting on the cross section which must be supplied by the joint are

$$\text{Shear} = + V/h$$

$$\text{Moment} = - \left(M_o + \frac{VL}{2}\right)/h$$

$$\text{Torque} = 0$$

The L.H.S. of the deflected shapre for $\delta_7 = 1$ has no components, as all the deflections are zero. The column in the matrix for loads of the second type for $\delta_7 = 1$ is given in Fig. 25.

For $\delta_6 = 1$, the component linear deflections are given in Fig. 26.

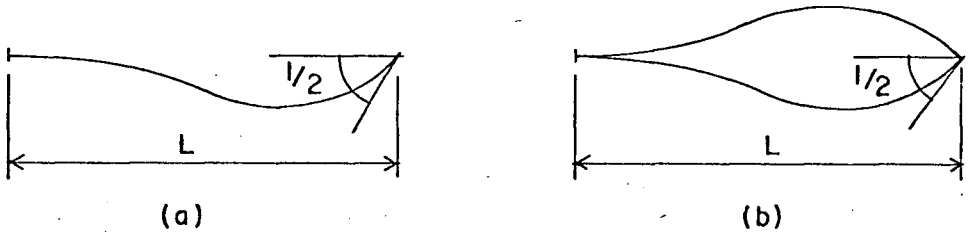


Fig. 26 COMPONENT DEFLECTIONS FOR $\delta_6 = 1$

Applying M, P and V, and taking their components along the allowed deflections gives:

(i) For the L.H.S. - no components, no forces.

(ii) For the R.H.S. - see Fig. 27.

| | 7 |
|---|---|
| 1 | 0 |
| 2 | 0 |
| 3 | 0 |
| 4 | 0 |
| 5 | $-\frac{(M_o + \frac{VL}{2})}{2h}$ |
| 6 | $-\frac{(M_o + \frac{VL}{2})}{2h}$ |
| 7 | $+\frac{V}{2h}$ |
| 8 | $+\frac{V}{2h}$ |

Fig. 25 TYPE 2 TERMS FOR NON-LINEAR MATRIX FOR $\delta_7 = 1$

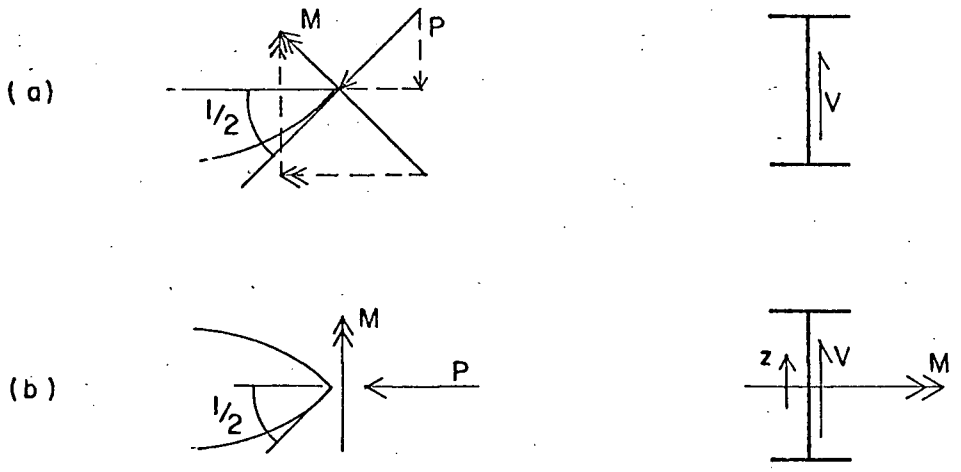


Fig. 27 FORCE COMPONENTS DUE TO END DEFLECTIONS FOR $\delta_6 = 1$

For Fig. 27(a) components acting along the allowed deflections are M/2, P/2. In stiffness matrix sign convention,

$$\text{Shear} = -P/2$$

$$\text{Moment} = 0$$

$$\text{Torque} = (M_o + VL/2)/2$$

For Fig. 27(b) the slope changes continuously from top to bottom. Therefore integration along the cross section must be used. Consider the effect of $\sigma$ at z on an element of area tdz, where

$$\sigma = +\frac{P}{A} - \frac{M_r z}{I_z} = \sigma_o - \frac{M_r z}{I_z}$$

$$\Delta \text{ force} = \sigma z t dz$$

slope @ z in x direction is z/h

Therefore, the component of force at z is $\frac{\sigma z t dz}{h}$

Integrating with respect to z to get the shear and torque gives

$$\text{Shear} = -\int_{z=-h/2}^{+h/2} \left(\frac{\sigma_o z t}{h} - \frac{M_r z^2 t}{I_z h}\right) dz = +\frac{M_r}{h} = \frac{M_o + VL/2}{h}$$

$$\text{Torque} = -\int_{z=-h/2}^{+h/2} \left(\frac{\sigma_o z^2 t}{h} - \frac{M_r z^3 t}{I_z h}\right) dz = -\frac{\sigma_o I_z}{h}$$

Because the flanges suffer the same angular displacements as the section as a whole, the end slopes of the flanges must be taken into account. See Fig. 28.

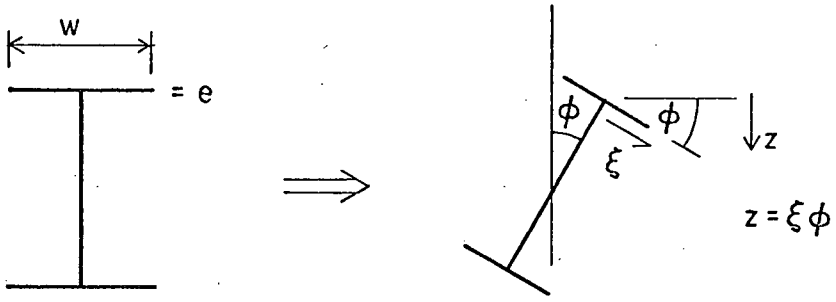


Fig. 28 VERTICAL FLANGE DEFLECTIONS AS FUNCTIONS OF $\phi$

The slope of the z deflection in the x direction in the flange is $\xi\phi' = \xi/h$ at point $\xi$. The differential force at point $\xi$ is

$$\Delta \text{ force} = \sigma e d\xi$$

The vertical shear component is

$$\int_{\xi=-w/2}^{+w/2} \left(\frac{\sigma_o e\xi}{h} - \frac{M_r h\xi e}{2I_z}\right) d\xi = 0$$

The torque is

$$-\int_{-w/2}^{+w/2}\left(\frac{\sigma_o e\xi^2}{h} - \frac{M_r h\xi^2 e}{2I_z}\right) d\xi = -\frac{\sigma_o I}{h} + \frac{M_r \xi^3 e}{6I_z}\Bigg|_{-w/2}^{+w/2}$$

However, the bottom flange has the same configuration with a moment stress on it of opposite sign. Therefore the net torque contribution of the flanges under moment stress is zero. However, the axial load contribution is the same for the bottom flange as for the top.

Therefore, the total contribution of the shape in Fig. 27(b) is given by

$$\text{Shear} = (M_o + VL/2)/h$$

$$\text{Moment} = 0$$

$$\text{Torque} = -2\frac{\sigma_o I}{h} - \frac{\sigma_o I_z}{h} = -\frac{\sigma_o I_p}{h}$$

After combining these forces, the column in the matrix for $\delta_6 = 1$ due to type two loads is given in Fig. 29. The remaining six columns can be found from similar calculations. This matrix, called $K_2$, can be written as

$$K_2 = Pk_{pz} + Mk_{m_2} + Vk_{v_2}$$

See Fig. 30.

The complete non-linear matrix for lateral torsional stability is given in Fig. 31 and is obtained by adding the matrices $K_1$ and $K_2$.

iv Numerical Examples

The matrix in Fig. 31 was used to calculate the critical loads of several structures, and the results were compared to the theoretical solutions.

A determinant plot method of solution was used. That is, the determinant of the structure matrix for increasing values of M, P and V were

| | 6 |
|---|---|
| 1 | 0 |
| 2 | 0 |
| 3 | 0 |
| 4 | 0 |
| 5 | 0 |
| 6 | 0 |
| 7 | $-\frac{P}{4} - \frac{\sigma_o I_p}{h^2} + \frac{M_o + \frac{VL}{2}}{2h} + \frac{M_o + \frac{VL}{2}}{2h}$ |
| 8 | $-\frac{P}{4} + \frac{\sigma_o I_p}{h^2} + \frac{M_o + \frac{VL}{2}}{2h} - \frac{M_o + \frac{VL}{2}}{2h}$ |

Fig. 29 TYPE 2 TERMS IN NON-LINEAR MATRIX FOR $\delta_6 = 1$

$Pk_{p_2} = P$

| | 1 | 2 | 3 | 4 | 5 | 6 | 7 | 8 |
|---|---|---|---|---|---|---|---|---|
| 1 | 0 | 0 | 0 | 0 | 0 | 0 | 0 | 0 |
| 2 | 0 | 0 | 0 | 0 | 0 | 0 | 0 | 0 |
| 3 | a - b | a + b | 0 | 0 | 0 | 0 | 0 | 0 |
| 4 | a + b | a - b | 0 | 0 | 0 | 0 | 0 | 0 |
| 5 | 0 | 0 | 0 | 0 | 0 | 0 | 0 | 0 |
| 6 | 0 | 0 | 0 | 0 | 0 | 0 | 0 | 0 |
| 7 | 0 | 0 | 0 | 0 | - a + b | - a - b | 0 | 0 |
| 8 | 0 | 0 | 0 | 0 | - a - b | - a + b | 0 | 0 |

$Mk_{m_2} = M_o(\frac{1}{hL})$

| | 1 | 2 | 3 | 4 | 5 | 6 | 7 | 8 |
|---|---|---|---|---|---|---|---|---|
| 1 | 0 | 0 | + L/2 | - L/2 | 0 | 0 | 0 | 0 |
| 2 | 0 | 0 | + L/2 | - L/2 | 0 | 0 | 0 | 0 |
| 3 | 0 | - L | 0 | 0 | 0 | 0 | 0 | 0 |
| 4 | + L | 0 | 0 | 0 | 0 | 0 | 0 | 0 |
| 5 | 0 | 0 | 0 | 0 | 0 | 0 | - L/2 | + L/2 |
| 6 | 0 | 0 | 0 | 0 | 0 | 0 | - L/2 | + L/2 |
| 7 | 0 | 0 | 0 | 0 | 0 | + L | 0 | 0 |
| 8 | 0 | 0 | 0 | 0 | - L | 0 | 0 | 0 |

$K_2 =$

$Vk_{v_2} = V(\frac{L}{12h})$

| | 1 | 2 | 3 | 4 | 5 | 6 | 7 | 8 |
|---|---|---|---|---|---|---|---|---|
| 1 | 0 | 0 | - 3 | + 3 | 0 | 0 | 0 | 0 |
| 2 | 0 | 0 | - 3 | + 3 | 0 | 0 | 0 | 0 |
| 3 | 0 | + 6 | - 6/L | + 6/L | 0 | 0 | 0 | 0 |
| 4 | - 6 | 0 | - 6/L | + 6/L | 0 | 0 | 0 | 0 |
| 5 | 0 | 0 | 0 | 0 | 0 | 0 | - 3 | + 3 |
| 6 | 0 | 0 | 0 | 0 | 0 | 0 | - 3 | + 3 |
| 7 | 0 | 0 | 0 | 0 | 0 | + 6 | + 6/L | - 6/L |
| 8 | 0 | 0 | 0 | 0 | - 6 | 0 | + 6/L | - 6/L |

$a = .1/4 \quad b = I_p/Ah^2$

Fig. 30 NON-LINEAR MATRIX FOR TYPE 2 LOADS

| | | 1 | 2 | 3 | 4 | 5 | 6 | 7 | 8 |
|---|---|---|---|---|---|---|---|---|---|
| P | 1 | 0 | 0 | 0 | 0 | 0 | 0 | 0 | 0 |
| | 2 | 0 | 0 | 0 | 0 | 0 | 0 | 0 | 0 |
| | 3 | 0 | 0 | -(a+b)/L | (-a+b)/L | 0 | 0 | (a+b)/L | (a-b)/L |
| | 4 | 0 | 0 | (-a+b)/L | -(a+b)/L | 0 | 0 | (a-b)/L | (a+b)/L |
| | 5 | 0 | 0 | 0 | 0 | 0 | 0 | 0 | 0 |
| | 6 | 0 | 0 | 0 | 0 | 0 | 0 | 0 | 0 |
| | 7 | 0 | 0 | (a+b)/L | (a-b)/L | 0 | 0 | -(a+b)/L | (-a+b)/L |
| | 8 | 0 | 0 | (a-b)/L | (a+b)/L | 0 | 0 | (-a+b)/L | -(a+b)/L |
| $M_o(\frac{1}{hL})$ | 1 | 0 | 0 | + L/2 | - L/2 | 0 | 0 | 0 | 0 |
| | 2 | 0 | 0 | + L/2 | - L/2 | 0 | 0 | 0 | 0 |
| | 3 | 0 | 0 | + 1 | 0 | 0 | 0 | - 1 | 0 |
| | 4 | 0 | 0 | 0 | - 1 | 0 | 0 | 0 | + 1 |
| | 5 | 0 | 0 | 0 | 0 | 0 | 0 | - L/2 | + L/2 |
| | 6 | 0 | 0 | 0 | 0 | 0 | 0 | - L/2 | + L/2 |
| | 7 | 0 | 0 | - 1 | 0 | 0 | 0 | + 1 | 0 |
| | 8 | 0 | 0 | 0 | + 1 | 0 | 0 | 0 | - 1 |
| $V(\frac{L}{12h})$ | 1 | 0 | 0 | - 3 | + 3 | 0 | 0 | 0 | 0 |
| | 2 | 0 | 0 | - 3 | + 3 | 0 | 0 | 0 | 0 |
| | 3 | + 1 | + 1 | - 6/L | 0 | - 1 | - 1 | 0 | + 6/L |
| | 4 | - 1 | - 1 | 0 | + 6/L | + 1 | + 1 | - 6/L | 0 |
| | 5 | 0 | 0 | 0 | 0 | 0 | 0 | - 3 | + 3 |
| | 6 | 0 | 0 | 0 | 0 | 0 | 0 | - 3 | + 3 |
| | 7 | - 1 | - 1 | 0 | - 6/L | + 1 | + 1 | + 6/L | 0 |
| | 8 | + 1 | + 1 | + 6/L | 0 | - 1 | - 1 | 0 | - 6/L |

$a = 1/4 \quad b = I_p/Ah^2$

Fig. 31 THE COMPLETE NON-LINEAR MATRIX FOR LOADS OF TYPE 1 AND 2

calculated and plotted. The value of M, P and V at which the determinant equalled zero was taken as the critical load. This technique was preferred to an eigenvalue approach since it avoids the problem of converging to a real eigenvalue which arises when an eigenvalue technique is applied to systems containing unsymmetric matrices.

A table of the results is given in Figs.32 and 32(a). A plot of the number of elements used against the accuracy obtained for four cases is given in Fig. 33.

The effect of applying vertical loads at points other than the centroid can be accounted for by modifying the stiffness matrix of the structure.

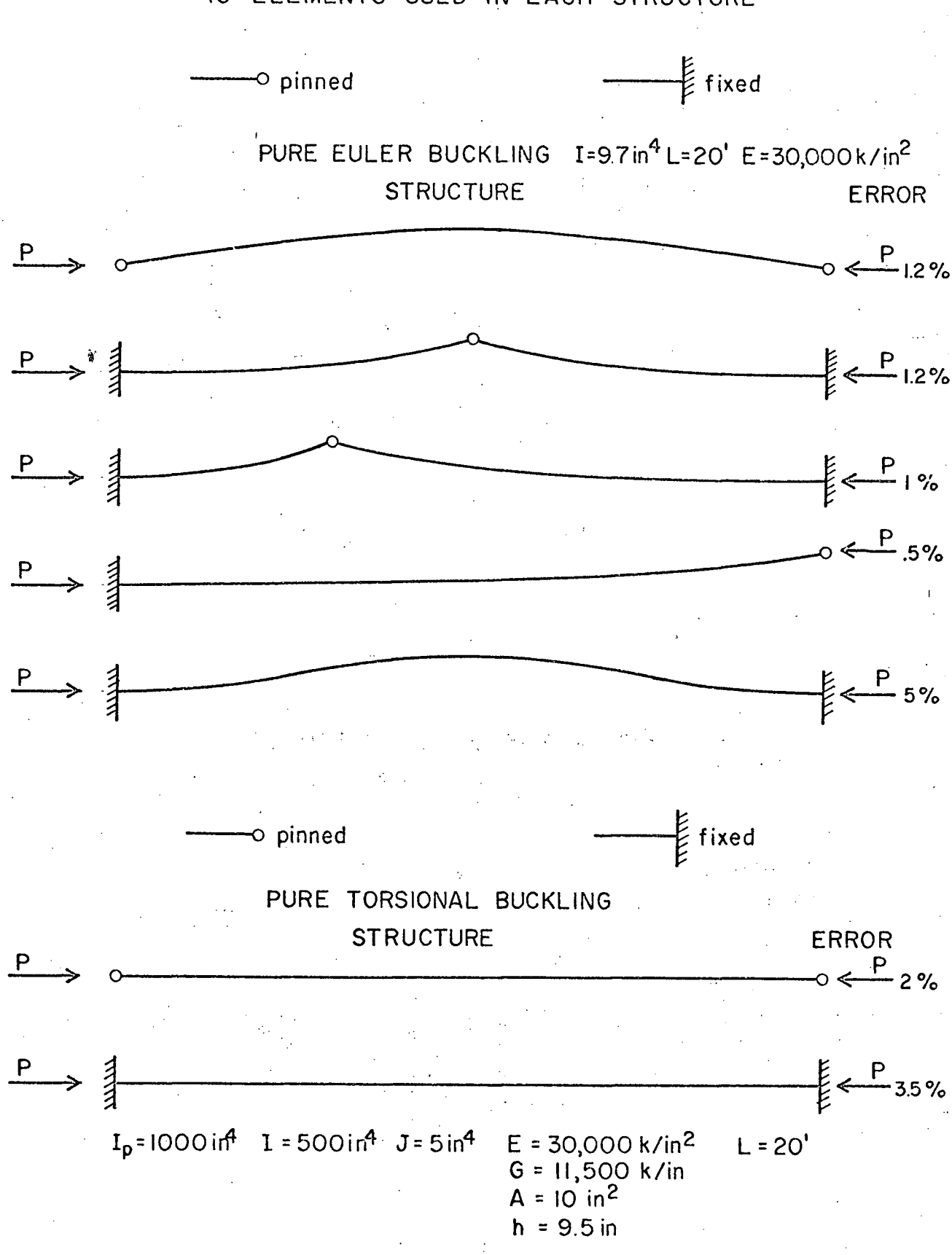


Fig. 32 TABLE OF RESULTS FOR TEST STRUCTURES

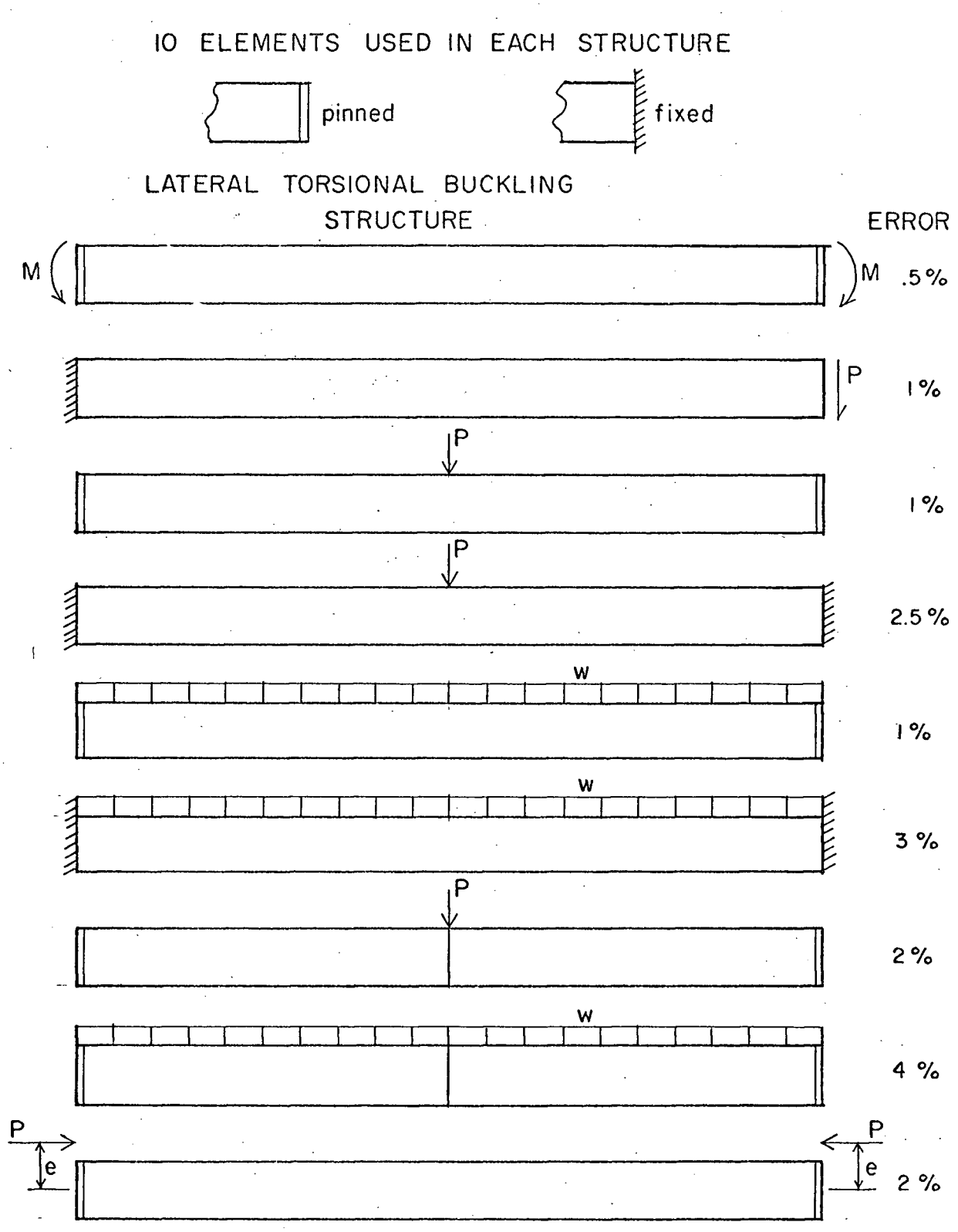


$I = 21\ in^4$ $I_p = 151\ in^4$ $A = 7.125\ in^2$ $J = .148\ in^4$ $E = 30{,}000\ k/in^2$
$G = 11{,}500\ k/in^2$

Fig. 32a TABLE OF RESULTS FOR TEST STRUCTURES

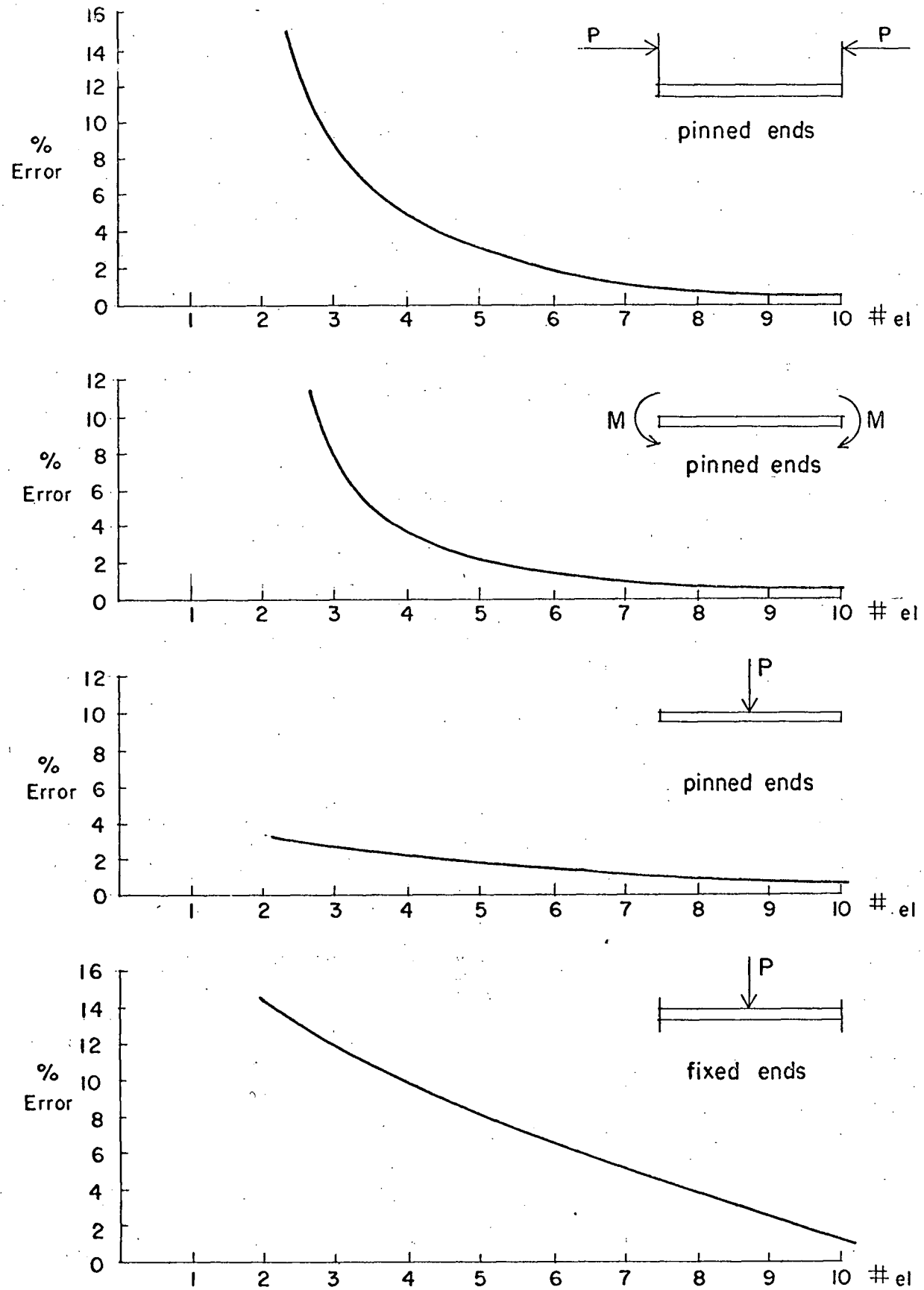


Fig. 33 PLOT OF ACCURACY VS. NUMBER OF ELEMENTS USED

# CHAPTER VII

## CONCLUSIONS

An 8 × 8 matrix for the exact linear treatment of doubly symmetric wide flange beams under torsion and lateral displacement was developed. This matrix allows each flange at either end to assume translations and rotations independent to the other flange.

An approximate matrix accounting for the effect of principal plane forces on the lateral deflections was developed. When added to the linear matrix, it makes possible the determination of the lateral-torsional buckling loads of wide flanged beams.

The non-linear matrix was based on small principal plane deflections and no distortion of the cross-section. Applied external loads must maintain their direction of application.

To obtain the non-linear stiffness matrix, differential equations were developed by considering a displaced element under the action of the principal forces. These were then solved to find the end forces which were entered in the matrix.

To ease the solution of the equation, a numerical technique was developed. This entailed substitution of the linear deflected shape into the R.H.S. of the differential equation to produce a known load, and then solving the L.H.S. for the new $y_1$ and $\phi_1$. The new deflections were $y_1$ and $\phi_1$ were then placed into the R.H.S. and the process repeated. The end conditions used were to be those of a fixed element. Effective end point loads acting due to the initial linear end deflections gave a second load set.

Two approximations were then utilized to further simplify the solution of the equations. The first entailed using only one cycle of the itera-

tion scheme. The second was to apply the effective lateral loads to an element with no end moment restraint.

Tests of the element against known solutions indicate that good accuracies can be obtained, but depend on the number of elements used in the analysis. Acceptable accuracies were obtained using ten elements, the largest error encountered being 5%.

The advantages of this matrix are several. Cases involving general load, support and end conditions of sections with varying section properties may now be solved by simply breaking the structure up into several elements and applying the presented matrix.

LIST OF REFERENCES


[1] Timoshenko, S.P., "Strength of Materials, Part II"
D. Van Nostrand Company, Inc., New York, N.Y. pp. 255-265, 1956

[2] Gere, J.M., and Weaver, W., "Analysis of Framed Structures"
D. Van Nostrand Company, Inc., New York, N.Y. pp. 430, 1965

[3] Timoshenko, S.P., and Gere, J.M., "Theory of Elastic Stability"
McGraw-Hill, Inc., New York, N.Y. pp. 251-270, 1961

[4] Bleich, F., "Buckling Strength of Metal Structures"
McGraw-Hill, Inc., New York, N.Y. pp. 149-160, 1952

[5] Timoshenko, S.P., "History of Strength of Material"
McGraw-Hill, Inc., New York, N.Y. pp. 393, 1953

[6] Goodier, J.N., "Some Observations on Elastic Stability"
Proceedings of the First National Congress of Applied Mechanics